中国石油大学(华东)
CHINA UNIVERSITY OF PETROLEUM

Theoretical study on nuclear structure by the electron-nucleus scattering

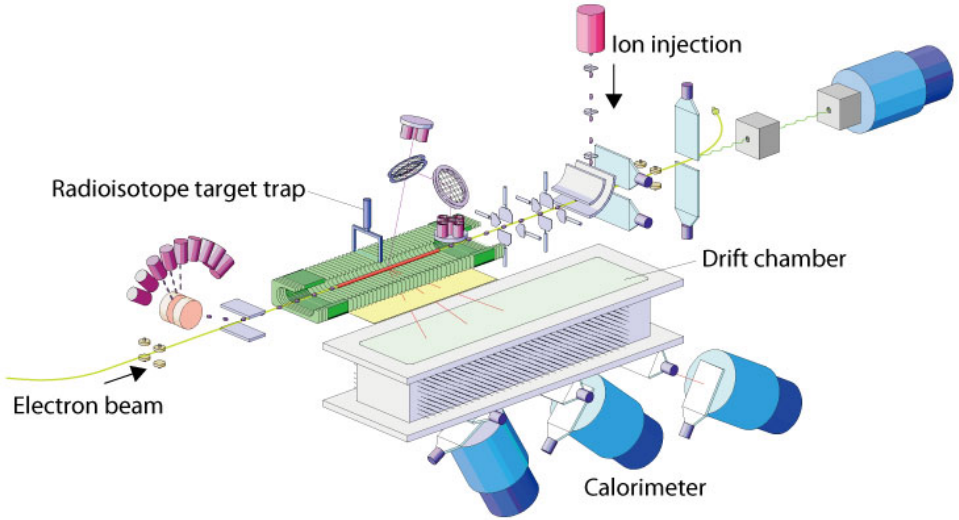

Jian Liu (刘健)

China University of Petroleum (East China)

2015. 7. 9

Content

- Introduction
- Relativistic mean-field model (RMF)
- Parity-violating electron scattering
- Electron scattering off deformed nuclei
- Summary and prospect

Sec. I Introduction

The observing capability of microscope is connected with the wave length of its probe.

Optical microscope
cellular scale (μm)
visible light 0.5 μm

Electron microscope
atomic scale(nm)
electrical energy 100keV
wavelength 0.004nm

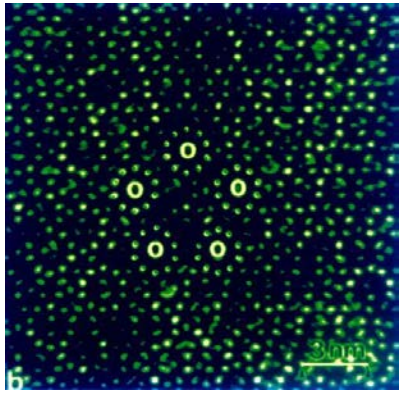

1.1 Elastic electron scattering

Effect method to measure at the nuclear scale:
High energy electron scattering

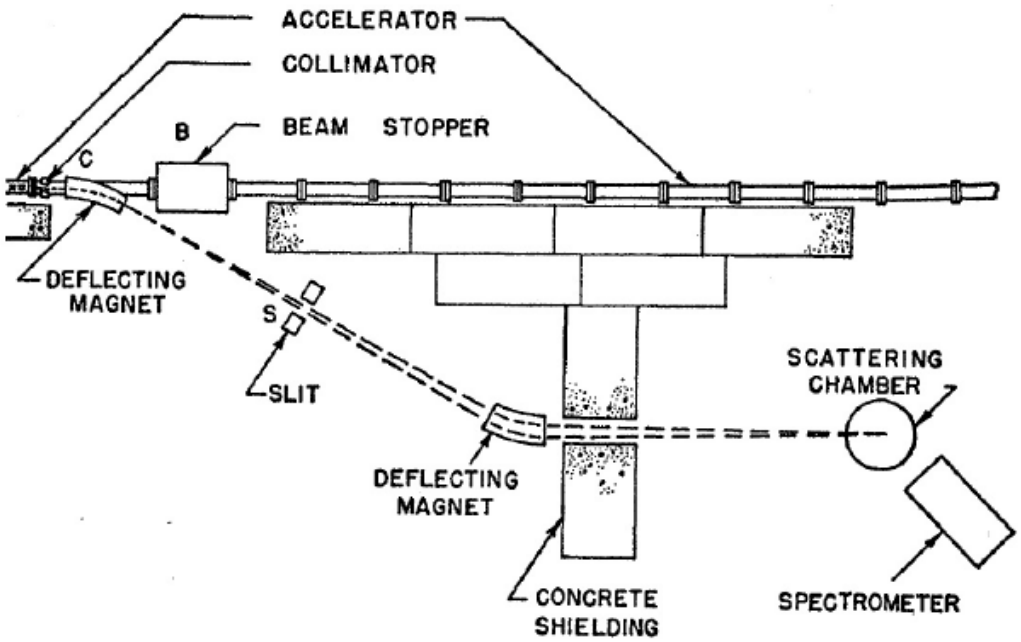

Experimental equipment of electron scattering (Hofstadter 1954)

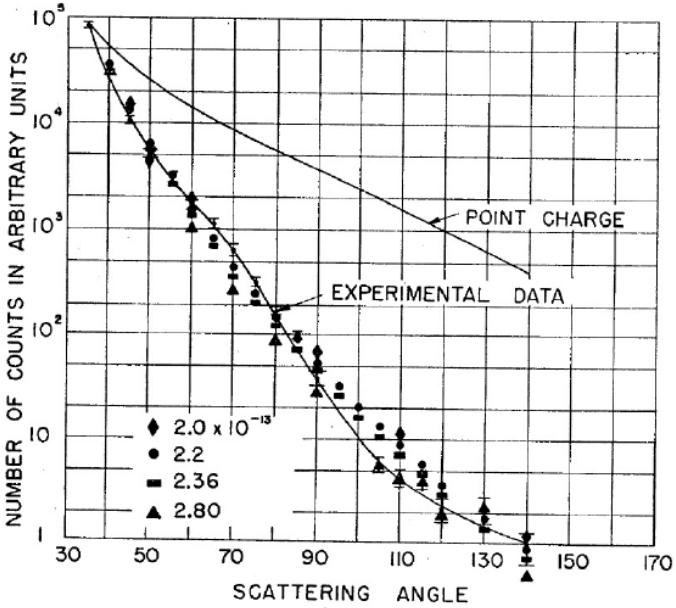

Hofstadter, R., et al., Phys. Rev. 92, 978 (1953).

Scattering cross section of electron

Theoretical development on electron scattering off nuclei

- 1911 Rutherford model of atom and Rutherford scattering formula
- 1929 Mott theory: electron scattering off point nuclei
- 1940s Guth, Rose: study the effect of nuclear size on electron scattering with the PWBA method.
- 1950s Hofstadter: experiments of high energy electron scattering off nuclei
- 1950s elastic electron scattering theories
  - Eikonal approximation
  - Phase-shift analysis method (DWBA)
- 1960s-1980s development's peak on the electron scattering experiments

Current situation of high energy electron scattering

With the development of radioactive ion beams, we could produce the exotic nuclei with short lives in the laboratory and investigate its structure now. With the new discovery of the nuclear properties, such as the halo nuclei, it raises the new questions about the nuclear structure.

Advantages of electron scattering:

The interaction between electron and nucleus is well understood.

Large scale facilities of electron scattering under construction:

- RIKEN of Japan
- GSI of Germany

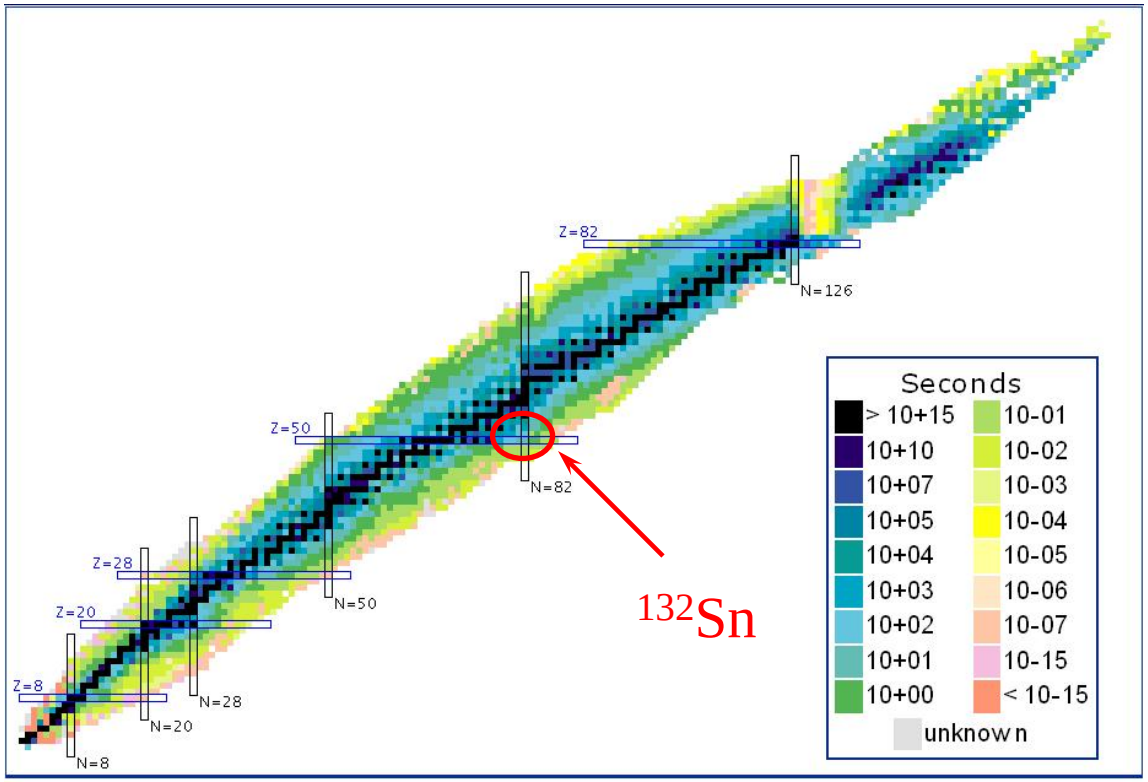

Experimental research progress on electron scattering

PRL **100,** 164801 (2008) PHYSICAL REVIEW LETTERS week ending 25 APRIL 2008

Novel Internal Target for Electron Scattering off Unstable Nuclei

M. Wakasugi,[1] T. Emoto,[1] Y. Furukawa,[2,*] K. Ishii,[3] S. Ito,[1] T. Koseki,[1,†] K. Kurita,[3] A. Kuwajima,[2] T. Masuda,[3,‡] A. Morikawa,[3] M. Nakamura,[1] A. Noda,[4] T. Ohnishi,[1] T. Shirai,[4] T. Suda,[1] H. Takeda,[1] T. Tamae,[2] H. Tongu,[4] S. Wang,[1] and Y. Yano[1]

[1]*RIKEN Nishina Center, Wako, Saitama 351-0198, Japan*
[2]*Laboratory of Nuclear Science, Tohoku University, Sendai, Miyagi 982-0826, Japan*
[3]*Department of Physics, Rikkyo University, Toshima, Tokyo 171-8501, Japan*
[4]*Institute of Chemical Research, Kyoto University, Uji, Kyoto 611-0011, Japan*
(Received 9 November 2007; published 22 April 2008)

RIKEN
Target project

PRL **102,** 102501 (2009) PHYSICAL REVIEW LETTERS week ending 13 MARCH 2009

First Demonstration of Electron Scattering Using a Novel Target Developed for Short-Lived Nuclei

T. Suda,[1] M. Wakasugi,[1] T. Emoto,[1] K. Ishii,[2] S. Ito,[1] K. Kurita,[2] A. Kuwajima,[3] A. Noda,[4] T. Shirai,[4,*] T. Tamae,[3] H. Tongu,[4] S. Wang,[1] and Y. Yano[1]

[1]*RIKEN Nishina Center, Wako, Saitama 351-0198, Japan*
[2]*Department of Physics, Rikkyo University, Toshima, Tokyo 171-8501, Japan*
[3]*Laboratory of Nuclear Science, Tohoku University, Sendai, Miyagi 982-0826, Japan*
[4]*Institute of Chemical Research, Kyoto University, Uji, Kyoto 611-0011, Japan*
(Received 10 October 2008; published 13 March 2009)

RIKEN
Verified experiment

1.2 Parity-violating electron scattering

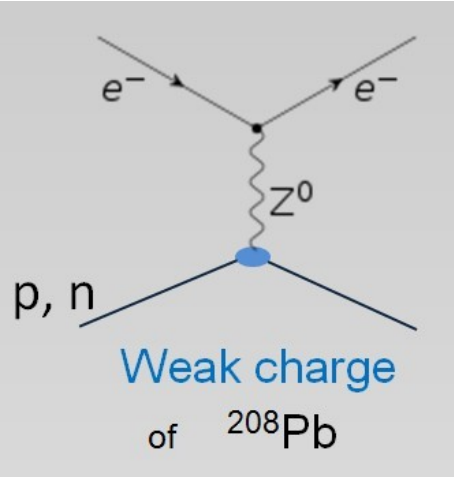

Z^0 is a good probe, which couples primary to neutron:

$$A = \frac{\left(\frac{d\sigma}{d\Omega}\right)_R - \left(\frac{d\sigma}{d\Omega}\right)_L}{\left(\frac{d\sigma}{d\Omega}\right)_R + \left(\frac{d\sigma}{d\Omega}\right)_L} = \frac{G_F Q^2}{2\pi\alpha\sqrt{2}}\left[1 - 4\sin^2\theta_W - \frac{F_N(Q^2)}{F_P(Q^2)}\right]$$

Taking into account the Coulomb distortion effects:

$$A = \frac{2\,\mathrm{Re}[M_\gamma^* M_Z]}{|M_\gamma|^2}$$

Parity-violating electron scattering (PVS) is considered to be a model independent method to probe the nuclear neutron properties, which was first proposed in 1989. **During the scattering process, the incident longitudinally polarized electrons interact with nucleons by exchanging either a photon or a Z^0 boson and the Z^0 boson couples primarily to neutrons**, which leads to the parity-violating experiment is sensitive to the neutron distribution.

The parity-violating electron scattering experiments at Jefferson Lab: PREx(^{208}Pb)、CREx(^{48}Ca)

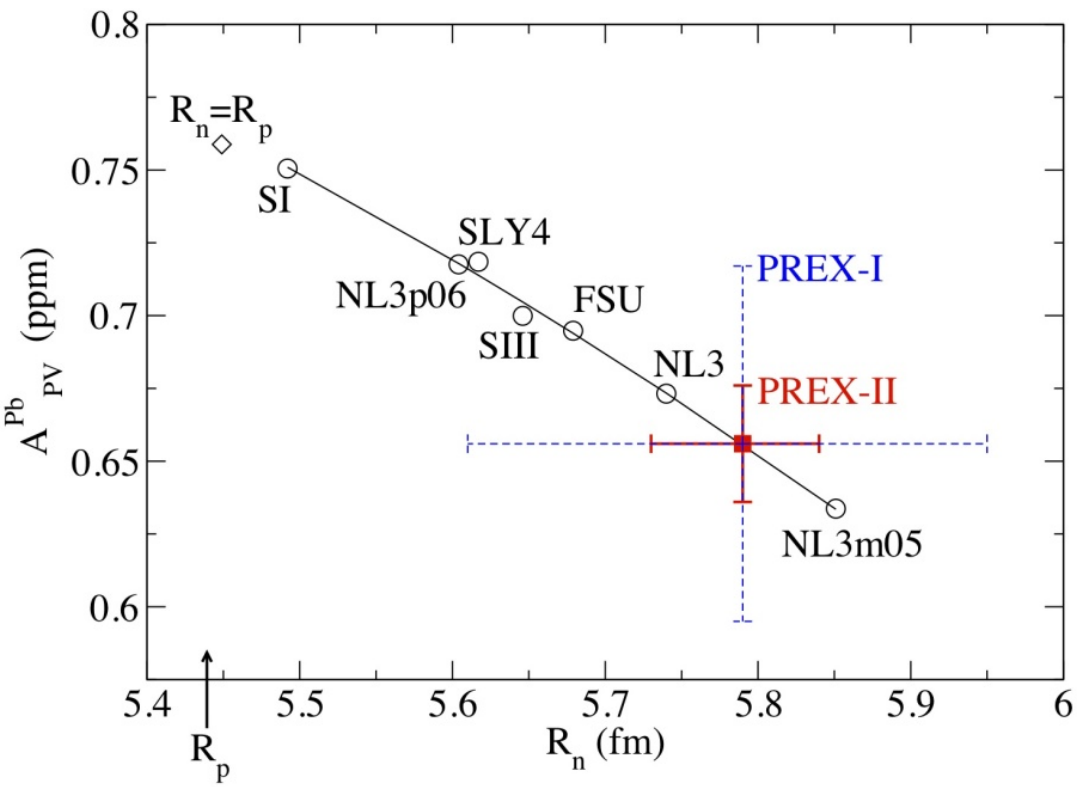

$$A_{pv} = 0.656 \text{ ppm} \pm 0.060(\text{stat}) \pm 0.014(\text{syst})$$

According to the measured Apv, the neutron skin is extracted to be:

$$R_{np} = R_n - R_p = 0.33^{+0.16}_{-0.18} \text{ fm}$$

$$\frac{dA}{A} = 3\% \quad \rightarrow \quad \frac{dR_n}{R_n} = 1\%$$

PREX-I Result
PRL 108 (2012) 112502
PRC 85 (2012) 03250(R)

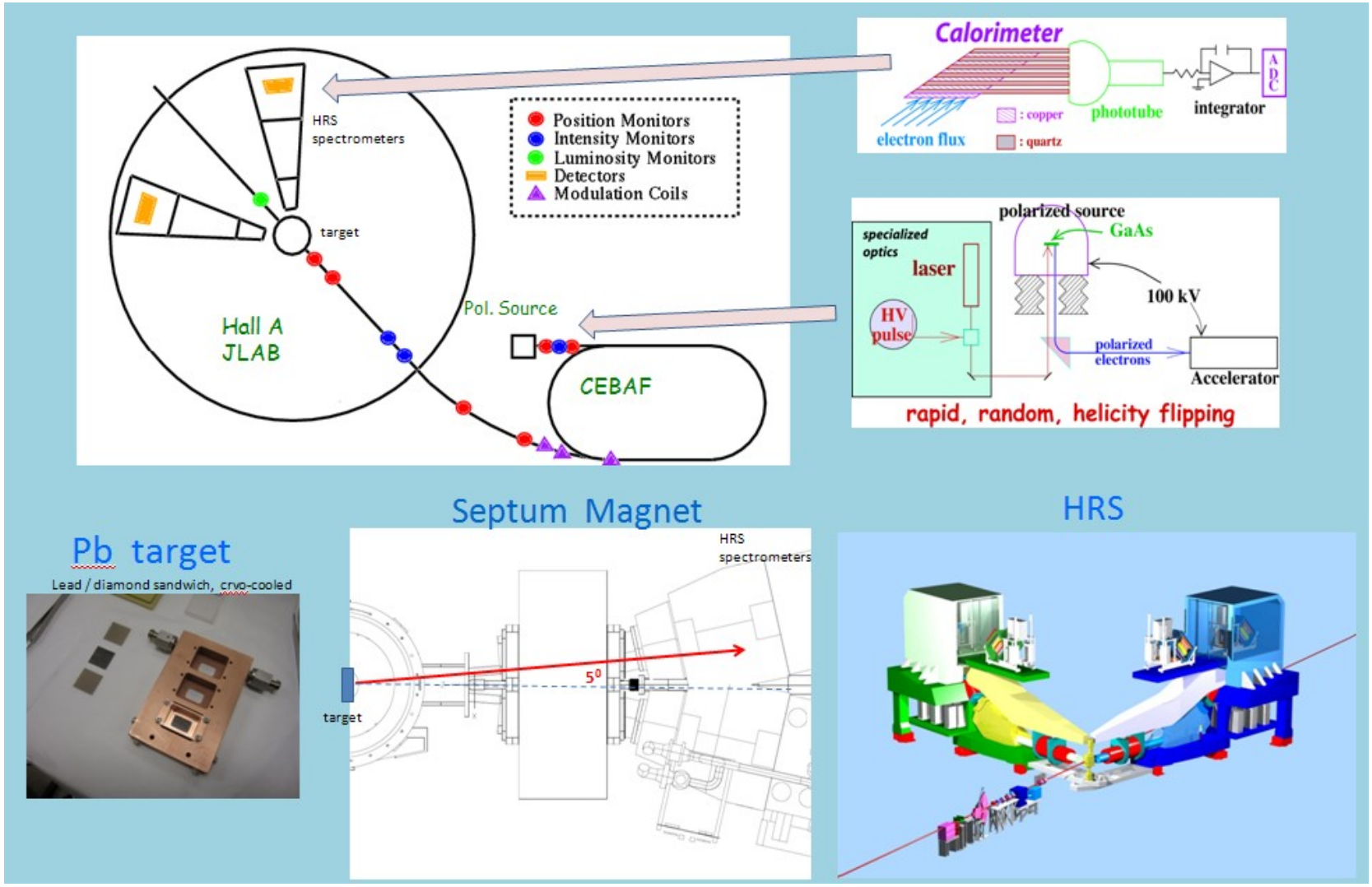

Experimental schematic of parity-violating electron scattering at JLab

Report content

The theoretical model of nuclear structure：

- **Relativistic mean-field model**

Theoretical method for electron scattering：

- **Plane-Wave Born approximation**
- **Eikonal approximation**
- **Phase-shift analysis**

Research subjects

- **Parity-violating electron scattering**
- **Electron scattering off deformed nuclei**

Sec. II Relativistic mean-field model

Lagrangian of relativistic mean-field model (RMF):

$$
\begin{aligned}
\mathcal{L} \;=\; & \bar{\Psi}(i\gamma^{\mu}\partial\mu - M)\Psi && \mathcal{L}_N \\
& -\bar{\Psi}(g_{\sigma}\sigma + g_{\omega}\gamma^{\mu}\omega_{\mu} + \frac{g_{\rho}}{2}\gamma^{\mu}\boldsymbol{\tau}\cdot\vec{\boldsymbol{\rho}}_{\mu})\Psi && \mathcal{L}_{couple} \\
& -e\bar{\Psi}\gamma^{\mu}A_{\mu}\frac{e}{2}(1-\tau_3)\Psi - \frac{1}{4}F^{\mu\nu}F_{\mu\nu} && \mathcal{L}_{\gamma} \\
& +\frac{1}{2}\partial^{\mu}\sigma\partial_{\mu}\sigma - \frac{1}{2}m_{\sigma}^2\sigma^2 - \frac{\kappa}{3!}(g_{\sigma}\sigma)^3 - \frac{\lambda}{4}(g_{\sigma}\sigma)^4 && \mathcal{L}_{\sigma} \\
& -\frac{1}{4}\Omega^{\mu\nu}\Omega_{\mu\nu} + \frac{1}{2}m_{\omega}^2\omega^{\mu}\omega_{\mu} + \frac{\xi}{4!}(g_{\omega}^2\omega^{\mu}\omega_{\mu})^2 && \mathcal{L}_{\omega} \\
& -\frac{1}{4}\vec{R}^{\mu\nu}\cdot\vec{R}_{\mu\nu} + \frac{1}{2}m_{\rho}^2\vec{\rho}^{\mu}\cdot\vec{\rho}_{\mu} && \mathcal{L}_{\rho} \\
& +\Lambda_{\mathrm{v}}(g_{\rho}^2\vec{\rho}^{\mu}\vec{\rho}_{\mu})(g_{\omega}^2\omega^{\mu}\omega_{\mu}) && \mathcal{L}_{\omega\rho}
\end{aligned}
$$

Apply the Euler-Lagrange equation to the wave function of nucleon：

$$\frac{\partial \mathcal{L}}{\partial \phi(x)} - \partial_\mu \frac{\partial \mathcal{L}}{\partial(\partial_\mu \phi)} = 0,$$

The Dirac equation for nucleon can be obtained:

$$\{-i\boldsymbol{\alpha}\cdot\nabla + \beta[M - S(\mathbf{r})] + U(\mathbf{r})\}\psi_i(\mathbf{r}) = \varepsilon_i \psi_i(\mathbf{r}),$$

where the scalar and vector potential is:

$$S(\mathbf{r}) = g_\sigma \sigma(\mathbf{r}),$$

$$U(\mathbf{r}) = g_\omega \omega_0(\mathbf{r}) + \frac{g_\rho}{2}\tau_3 \rho_0(\mathbf{r}) + \frac{e}{2}(1-\tau_3)A_0(\mathbf{r}).$$

The Dirac spinor of nucleon:

$$\psi_{\alpha,\kappa,m}(\mathbf{r},s,t) = \begin{pmatrix} i\frac{G_\alpha^\kappa(r)}{r}Y_{jm}^{l}(\theta,\phi,s) \\ -\frac{F_\alpha^\kappa(r)}{r}Y_{jm}^{\tilde{l}}(\theta,\phi,s) \end{pmatrix}\chi_{t_\alpha}(t), \qquad j = l \pm \frac{1}{2},$$

where n is the principle quantum number;

m is the magnetic quantum number;

s is the spin and t is the isospin

$Y_{jm}^{l}(\theta,\phi,s)$ 为二维的自旋球谐函数，其定义为：

$$Y_{jm}^{l}(\theta,\phi,s) = \sum_{m_s,m_l}\langle\frac{1}{2}m_s l m_l|jm\rangle Y_{lm}(\theta,\phi)\chi_{m_s}(s)$$

Substituting the Dirac spinors into the Dirac equation of nucleon, the equations for radical wave function of nucleon can be obtained:

$$\varepsilon_\alpha G_\alpha^\kappa = \left(-\frac{\partial}{\partial r} + \frac{\kappa}{r}\right) F_\alpha^\kappa + (M + S(r) + U(r)) G_\alpha^\kappa,$$

$$\varepsilon_\alpha F_\alpha^\kappa = \left(+\frac{\partial}{\partial r} + \frac{\kappa}{r}\right) G_\alpha^\kappa - (M + S(r) - U(r)) F_\alpha^\kappa.$$

The nuclear densities can be obtained from the radical wave functions:

$$4\pi r^2 \rho_s(r) = \sum_{i=1}^{A} (|G_i(r)|^2 - |F_i(r)|^2),$$

$$4\pi r^2 \rho_v(r) = \sum_{i=1}^{A} (|G_i(r)|^2 + |F_i(r)|^2),$$

$$4\pi r^2 \rho_3(r) = \sum_{i=1}^{A} 2\tau_{3i} (|G_i(r)|^2 + |F_i(r)|^2),$$

$$4\pi r^2 \rho_p(r) = \sum_{i=1}^{A} (\frac{1}{2} - \tau_{3i}) (|G_i(r)|^2 + |F_i(r)|^2).$$

Apply the Euler-Lagrange equation to the wave functions of meson, the equations of motion for mesons and photon can be obtained:

$$
\begin{aligned}
&(-\Delta + m_\sigma^2)\sigma(\mathbf{r}) = g_\sigma \rho_s(\mathbf{r}) - \frac{\kappa}{2} g_\sigma^3 \sigma^2(\mathbf{r}) - \frac{\lambda}{6} g_\sigma^4 \sigma^3(\mathbf{r}), \\
&(-\Delta + m_\omega^2)\omega(\mathbf{r}) = g_\omega \rho_{\mathrm{v}}(\mathbf{r}) - \frac{\zeta}{6} g_\omega^4 \omega_0^3(\mathbf{r}) - 2\Lambda_{\mathrm{v}} g_\rho^2 g_\omega^2 \rho_0^2(\mathbf{r})\omega_0(\mathbf{r}), \\
&(-\Delta + m_\rho^2)\rho_0^2(\mathbf{r}) = \frac{g_\rho}{2}\rho_3(\mathbf{r}) - 2\Lambda_{\mathrm{v}} g_\omega^2 g_\rho^2 \omega_0^2(\mathbf{r})\rho_0(\mathbf{r}), \\
&-\Delta A_0(\mathbf{r}) = e\rho_p(\mathbf{r}),
\end{aligned}
$$

The nuclear energy in the RMF model:

$$E = E_{nucleon} + E_\sigma + E_\omega + E_\rho + E_{coulomb} + E_{cm}$$

The expression for each item:

$$\begin{cases} E_{nucleon} = \sum_{i=1}^{A} \varepsilon_i \\ E_\sigma = -\frac{1}{2}\int_V d^3r\,(g_\sigma \sigma(\boldsymbol{r})\rho_s(\boldsymbol{r}) + U(\sigma)) \\ E_\omega = -\frac{1}{2}\int_V d^3r\, g_\omega \omega(\boldsymbol{r})\rho_v(\boldsymbol{r}) \\ E_\rho = -\frac{1}{2} g_\rho \boldsymbol{\rho}(\boldsymbol{r})\left(\rho_v^{(p)}(\boldsymbol{r}) - \rho_v^{(n)}(\boldsymbol{r})\right) \\ E_{Coulomb} = -\frac{1}{2}\int_V d^3 A_0 \rho_v^{(p)}(\boldsymbol{r}) \\ E_{cm} = -\frac{3}{4} \times 41 \times A^{1/3} \end{cases}$$

TABLE II. Experimental data for the binding energy per nucleon (in MeV) [60] and charge radius (in fm) [61] for all the nuclei involved in the optimization. Also displayed are the theoretical results obtained with NL3 [8], FSUGold [10], and FSUGold2.

Nucleus	Observable	Experiment	NL3	FSU	FSU2
^{16}O	B/A	7.98	8.06	7.98	8.00
	R_{ch}	2.70	2.75	2.71	2.73
^{40}Ca	B/A	8.55	8.56	8.54	8.54
	R_{ch}	3.48	3.49	3.45	3.47
^{48}Ca	B/A	8.67	8.66	8.58	8.63
	R_{ch}	3.48	3.49	3.48	3.47
^{68}Ni	B/A	8.68	8.71	8.66	8.69
	R_{ch}	—	3.88	3.88	3.86
^{90}Zr	B/A	8.71	8.70	8.68	8.69
	R_{ch}	4.27	4.28	4.27	4.26
^{100}Sn	B/A	8.25	8.30	8.24	8.28
	R_{ch}	—	4.48	4.48	4.47
^{116}Sn	B/A	8.52	8.50	8.50	8.49
	R_{ch}	4.63	4.63	4.63	4.61
^{132}Sn	B/A	8.36	8.38	8.34	8.36
	R_{ch}	4.71	4.72	4.74	4.71
^{144}Sm	B/A	8.30	8.32	8.32	8.31
	R_{ch}	4.95	4.96	4.96	4.94
^{208}Pb	B/A	7.87	7.90	7.89	7.88
	R_{ch}	5.50	5.53	5.54	5.51

Sec. III Parity-violating electron scattering

The physical picture of electron scattering:

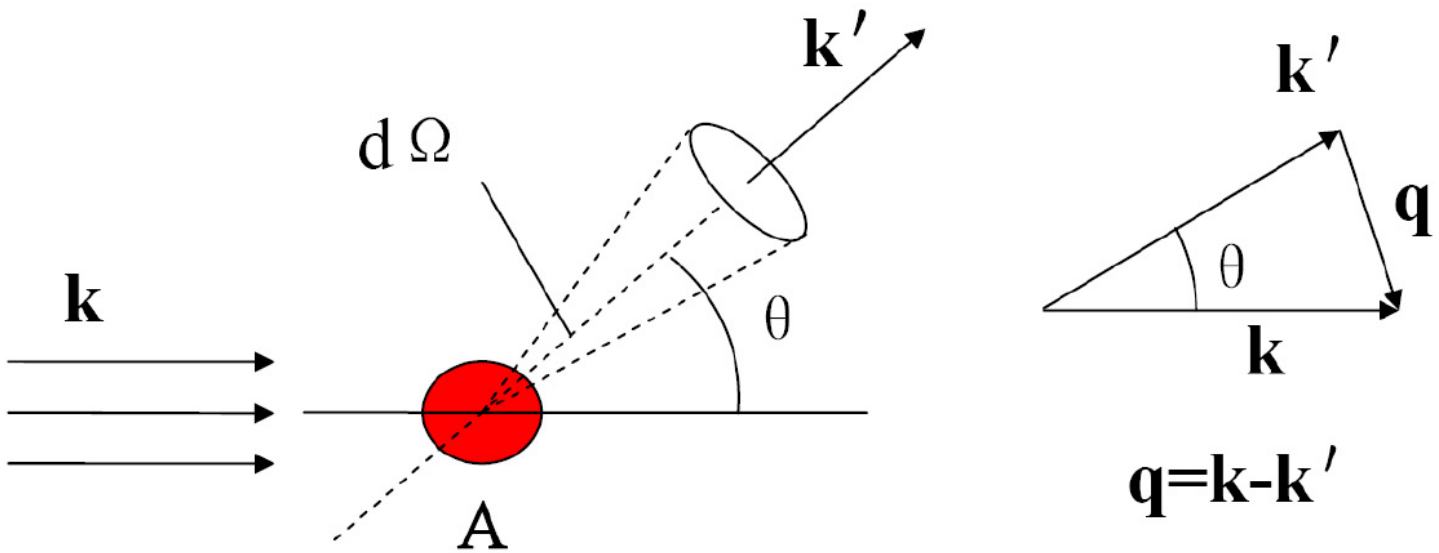

The purpose of theoretical study:

Calculating the scattering probability of electron in one solid angle, which is the scattering differential cross section.

2.1 Theoretical methods for electron scattering

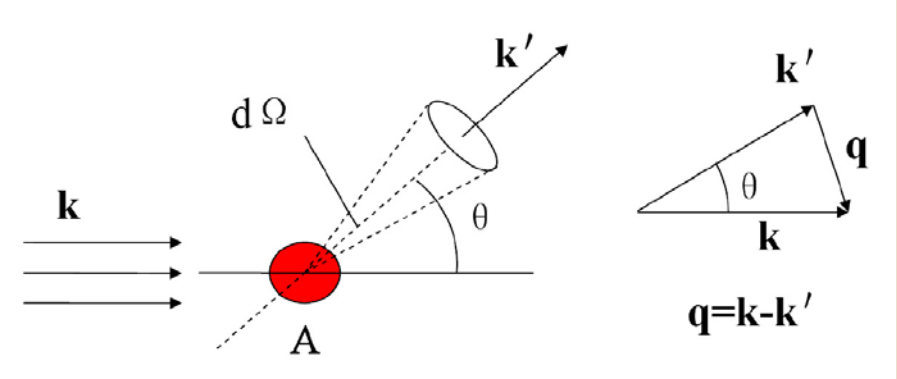

1. Plane wave Born approximation (PWBA)

The wave function of incident electron is the plane wave, which is eigenfunction of Hamiltonian of free electron $\hat{H}_0 = \hat{P}^2/2m$. The wave function of scattered electron is $|\Psi^+\rangle$。

The differential cross section:

$$\frac{d\sigma}{d\Omega} = |f(\theta)|^2 \qquad f(\theta) = -\frac{1}{4\pi}(2\pi)^3 \frac{2m}{\hbar^2}\langle \Psi_{\mathbf{k}} | V | \Psi^+ \rangle$$

If the effect of target nuclei are not very big, the wave function of scattering can also be seen as the plane wave $|\phi\rangle$。 The application condition of PWBA is the energy of incident electron is high enough and influence of target nuclei is weak.

Eikonal approximation

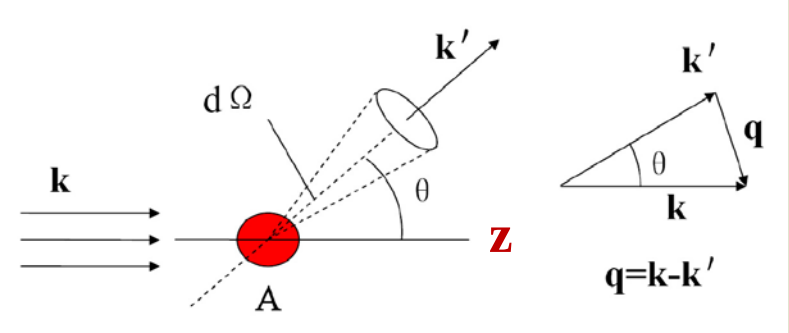

If the energy of incident electron is high and scattering angle is not large, the particle behavior of electron is strong. The semiclassical path concept is applicable. The wave function of scattering electron can be replace by the semiclassical wave function $\Psi^{(+)} \sim e^{iS(x)/\hbar}$. For the situation $E \gg |V|$, we can obtain:

$$\Psi^{(+)}(\mathbf{x}) = \Psi^{(+)}(\mathbf{b} + z\hat{\mathbf{z}}) \simeq \frac{1}{(2\pi)^{3/2}} e^{ikz} \exp\left[\frac{-im}{\hbar^2 k} \int_{-\infty}^{z} V\left(\sqrt{b^2 + z'^2}\right) \mathrm{d}z'\right].$$

From the equation, we can see that the wave function $\Psi^{(+)}$ is divided into two parts: one is e^{ikz} , which is the wave function of incident electron; the other is $\exp\left[\frac{-im}{\hbar^2 k} \int_{-\infty}^{z} V\left(\sqrt{b^2 + z'^2}\right) \mathrm{d}z'\right]$, which is the influence of Coulomb field of target nuclei.

Phase-shift analysis method (DWBA)

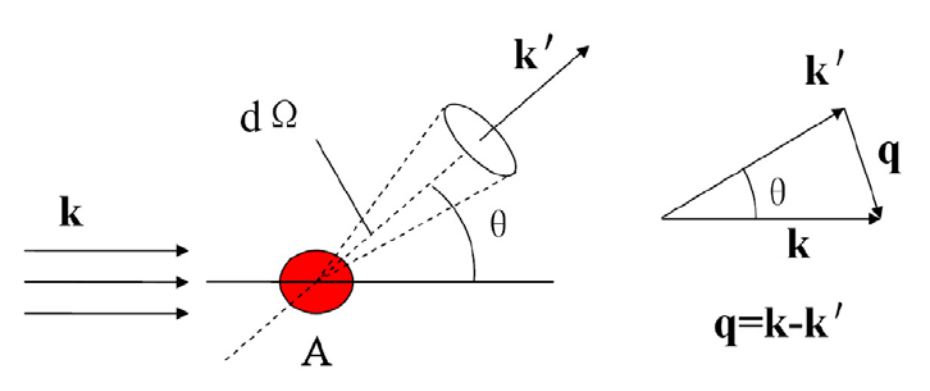

Another method to deal with the Coulomb distortion is the phase-shift analysis method which expands the wave function of scattered electron to the sum of components of angular momentum.

$$\Psi(\mathbf{r}) = e^{i\mathbf{k}\cdot\mathbf{z}} + f(\theta,\phi)\frac{e^{i\mathbf{k}\cdot\mathbf{r}}}{r}$$

$$= \sum_l (2l+1) i^l R_l(r) P_l(\cos\theta)$$

where $R_l(r)$ is the radial wave function of scattered electron. $P_l(\cos\theta)$ is the Lengendre polynomials.

Every wave functions with angular momentum l have contributions to the scattering amplitude. The total scattering amplitude can be obtained by the sum of the scattering amplitude in l order.

Detailed formulas for phase-shift analysis method:

- Dirac equation of electron $\left[\boldsymbol{\alpha}\cdot\mathbf{p}+\beta m+V(r)\right]\psi(\mathbf{r})=E\psi(\mathbf{r})$

  Coulomb potential $V_c(\mathbf{r})=-\dfrac{e^2}{4\pi\epsilon_0}\displaystyle\int\frac{\rho_c(\mathbf{r}')}{|\mathbf{r}-\mathbf{r}'|}d\mathbf{r}'$

- If V(r) is symmetric, the wave functions can be described with Dirac spinor:

$$\psi_{\kappa m_j}(\mathbf{r})=\frac{1}{r}\begin{bmatrix} P(r)\Omega_{\kappa,m_j}(\theta,\phi) \\ iQ(r)\Omega_{-\kappa,m_j}(\theta,\phi)\end{bmatrix}$$

- Expansion coefficents P(r),Q(r) satisfy:

$$\frac{dP}{dr}=-\frac{\kappa}{r}P(r)+[E-V(r)+2m]Q(r),$$
$$\frac{dQ}{dr}=-[E-V(r)]P(r)+\frac{\kappa}{r}Q(r).$$

- Combining the boundary conditions, the phase-shift analysis $\delta_l^{\pm}$ can be obtained.

The asymptotic behavior of the wave function:

$$r \to \infty \qquad j_l(r) \to \frac{\mathrm{Sin}(kr - l\frac{\pi}{2})}{kr}$$

$$\frac{dP}{dr} = -\frac{\kappa}{r}P(r) + [E - V(r) + 2m]Q(r),$$
$$\frac{dQ}{dr} = -[E - V(r)]P(r) + \frac{\kappa}{r}Q(r).$$

$$P_{E\kappa}(r) \to \mathrm{Sin}(kr - l\frac{\pi}{2} - \eta \ln 2kr + \Delta_\kappa)$$

$$Q_{E\kappa}(r) \to \mathrm{Cos}(kr - l\frac{\pi}{2} - \eta \ln 2kr + \Delta_\kappa)$$

Direct scattering amplitude

$$g(\theta) = \frac{1}{2ik} \sum_{l=0}^{\infty} \left[e^{2i\delta_l^-} - e^{2i\delta_l^+} \right] P_l^1(\cos\theta)$$

Spinflip scattering amplitude

$$f(\theta) = \frac{1}{2ik} \sum_{l=0}^{\infty} \left[(l+1)(e^{2i\delta_l^+} - 1) + l(e^{2i\delta_l^-} - 1) \right] P_l(\cos\theta)$$

Cross section:

$$\frac{d\sigma}{d\Omega} = |f(\theta)|^2 + |g(\theta)|^2$$

Charge form factor:

$$|F(q)|^2 = \frac{d\sigma/d\Omega}{d\sigma_M/d\Omega}$$

where Mott cross section is:

$$\frac{d\sigma_M}{d\Omega} = \left(\frac{Z\alpha^2}{2E} \right)^2 \frac{\cos^2\frac{\theta}{2}}{\sin^4\frac{\theta}{2}}$$

The comparison between the experimental data and theoretical calculations of DWBA

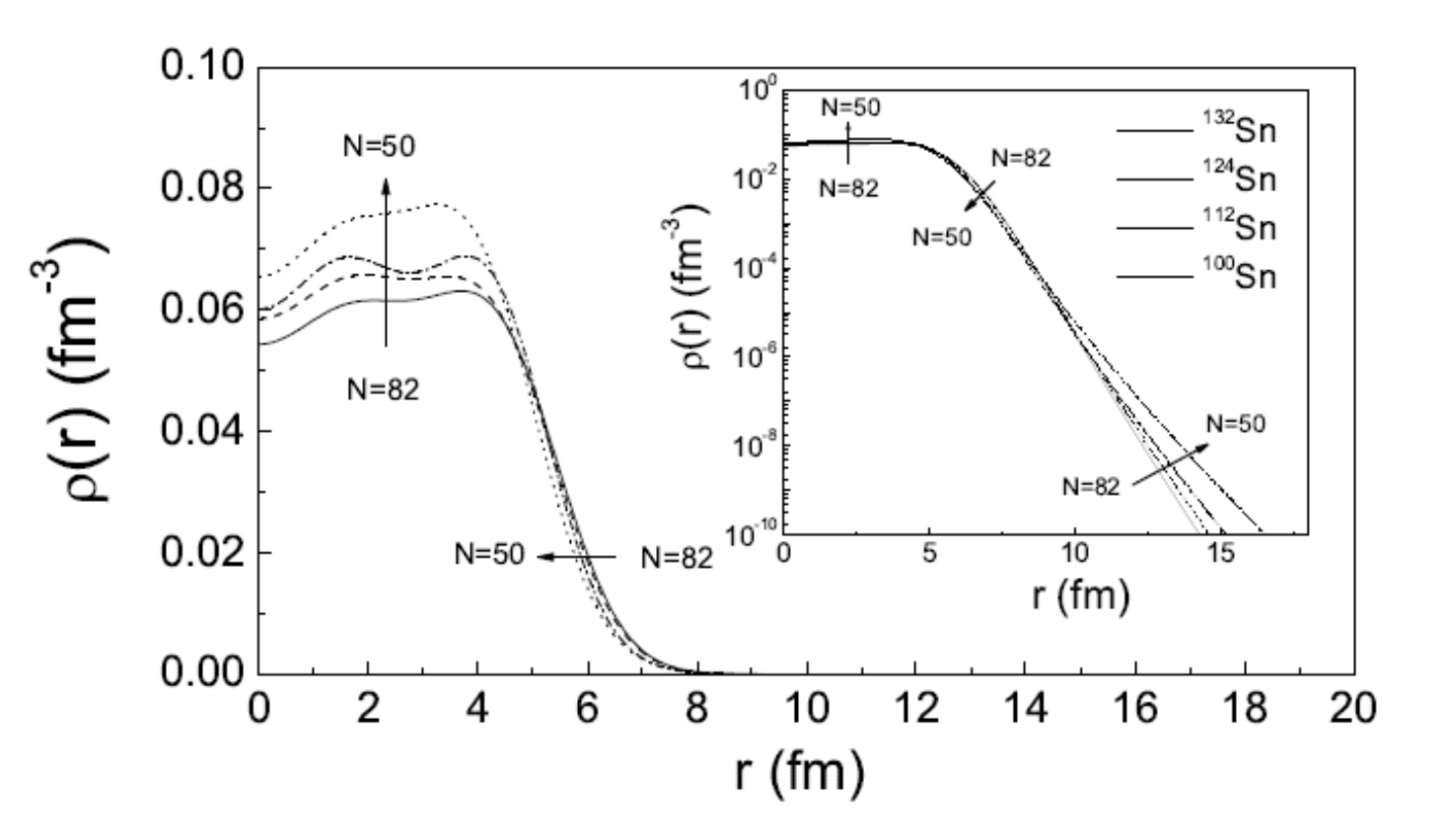

The charge density distributions of Sn isotopes from the RMF model

With the decrease of the neutron number, the spatial extension becomes larger.

J. Liu and Z. Ren, *Nucl. Phys. A* **888**, 45 (2012).

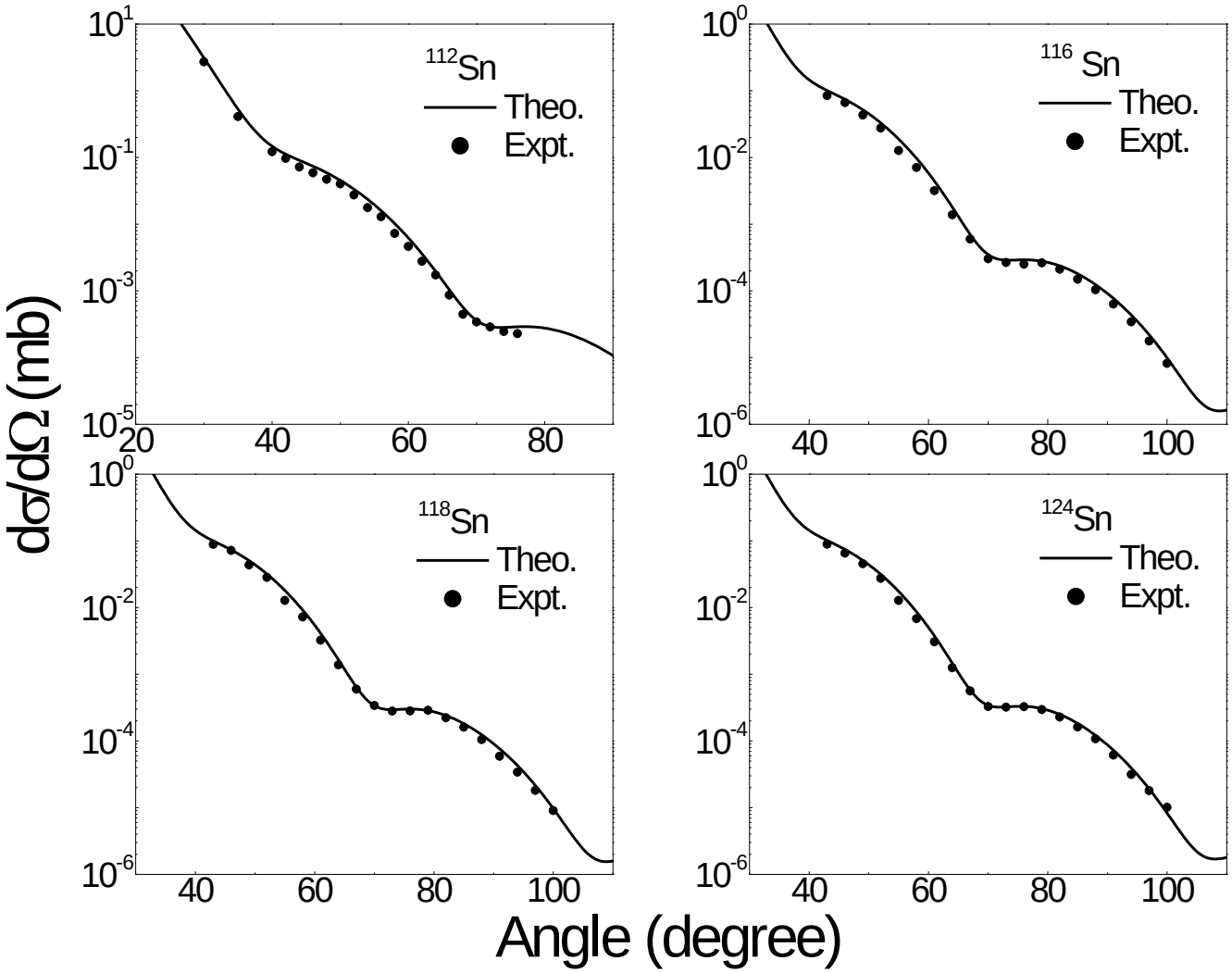

Elastic cross sections of Sn isotopes

J. Liu and Z. Ren, *Nucl. Phys. A* **888**, 45 (2012).

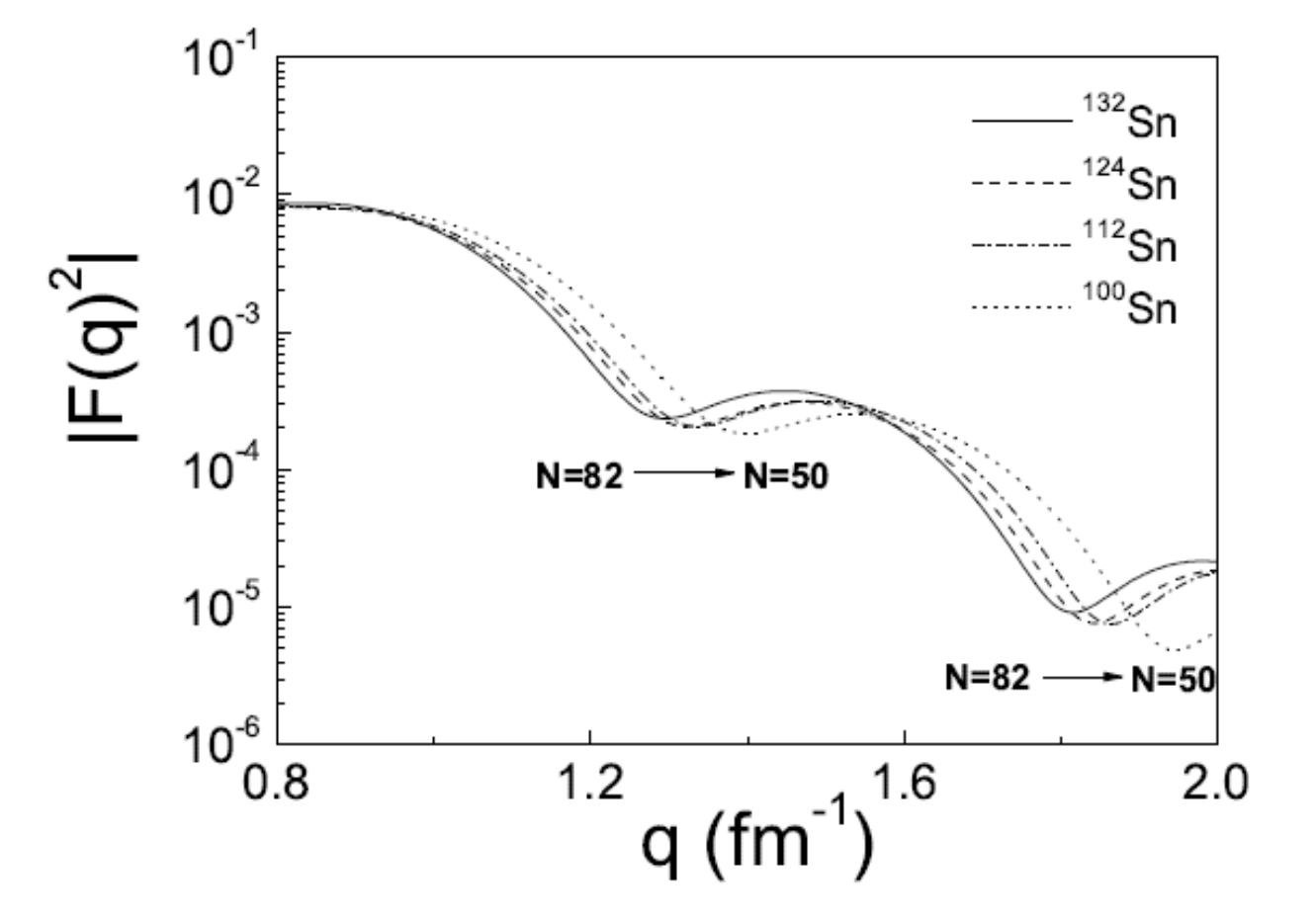

Elastic charge form factors of Sn isotopes

With the increase of the neutron number, the minima of the charge form factor shift inside and upside.

3.2 Theoretical framework of parity-violating electron scattering

Research background

- Neutron, being electrically neutral particles, cannot be measured from the elastic electron scattering. The experiments with hadronic probes always have large error bars and the interpretation is model-dependent.

- The meanings of accurate neutron distribution.
  - The input of neutron reaction model.
  - Testing the nuclear structure model.

- In 1989, Donnelly, Dubach and Sick propose the parity-violating electron scattering to study the neutron density distribution.

- The Coulomb and weak interaction between the electron and nucleus.
- The potential for electron with positive and negative parity is different

$$\frac{\boldsymbol{\sigma}\cdot\mathbf{p}}{|\mathbf{p}|}=+1, \qquad V_+(r)=V_C(r)+A(r)$$

$$\frac{\boldsymbol{\sigma}\cdot\mathbf{p}}{|\mathbf{p}|}=-1, \qquad V_-(r)=V_C(r)-A(r)$$

Coulomb potential **Weak potential**

Weak potential: $A(r)=\frac{G_F}{2\sqrt{2}}\rho_W(r)$

about 0.08

Weak density:

$$\rho_W(r)=\int d^3r' G_E\left(|\mathbf{r}-\mathbf{r}'|\right)\left[\boxed{(1-4\sin^2\theta_W)}\rho_p(\mathbf{r}')-\rho_n(\mathbf{r}')\right]$$

The neutron contribute to the weak potential dominantly.

During the scattering process, the wave function of polarized electron can be divided into two parts: $\Psi = \Psi_+ + \Psi_-$ where $\Psi_\pm = \frac{1}{2}(1 \pm \gamma_5)\Psi$.

They satisfy the Dirac equation:

$$\left[\boldsymbol{\alpha} \cdot \mathbf{p} + V_\pm(r)\right]\Psi_\pm = E\Psi_\pm$$

- **The parity-violating asymmetries:** $A_{\mathrm{pv}} = \dfrac{\mathrm{d}\sigma_+ / \mathrm{d}\Omega - \mathrm{d}\sigma_- / \mathrm{d}\Omega}{\mathrm{d}\sigma_+ / \mathrm{d}\Omega + \mathrm{d}\sigma_- / \mathrm{d}\Omega}$

$d\sigma_+ / d\Omega$ and $d\sigma_- / d\Omega$ are cross sections of positive and negative electrons, respectively.

Under the PWBA method, the parity-violating asymmetry can written as:

$$A_{\mathrm{pv}} = \frac{G_F q^2}{4\pi\sqrt{2}\alpha}\left[\frac{F_n(q)}{F_p(q)} + 4\sin^2\theta_W - 1\right]$$

Comparison betwen the PWBA and DWBA method

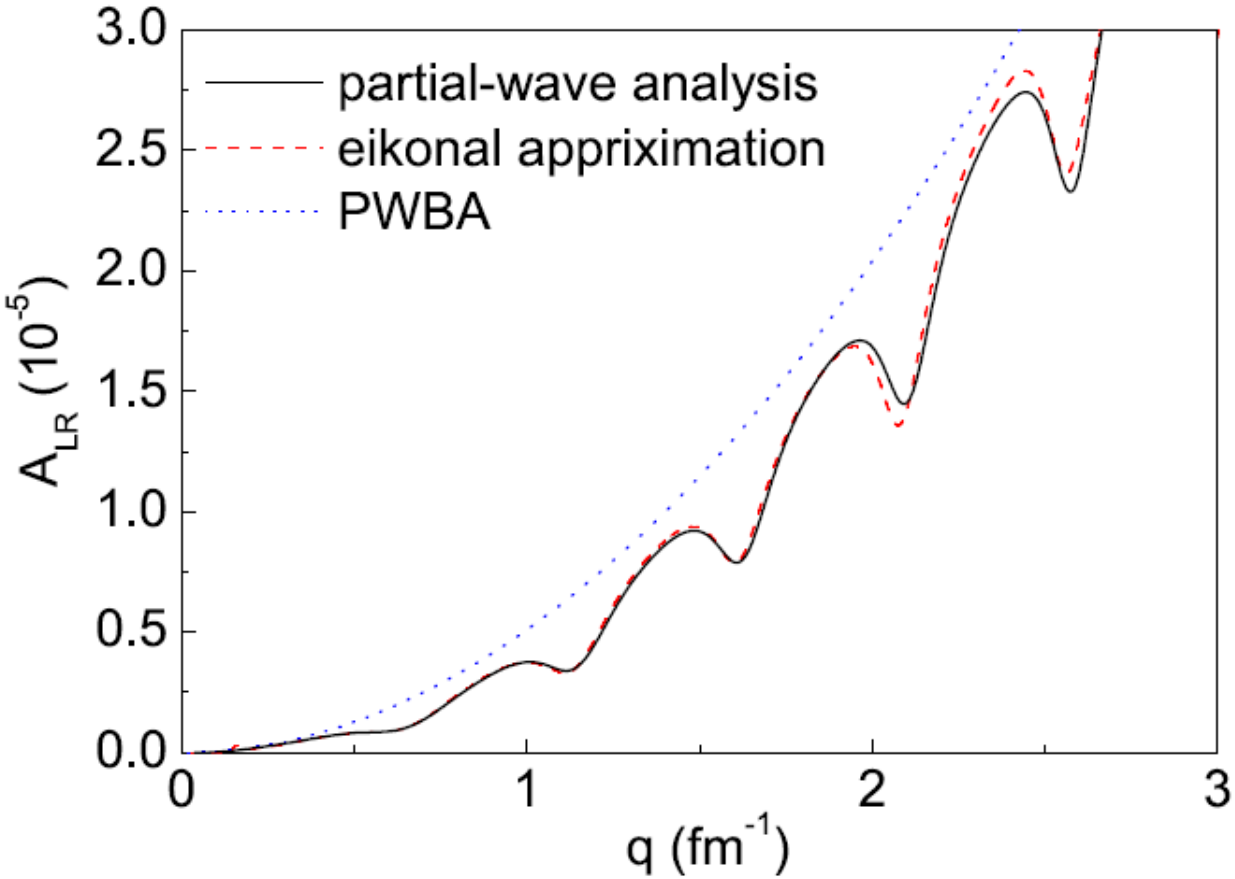

^{208}Pb 850MeV Calculated with different method.

PWBA method can give the right changing trend. The results of Eikonal approximation and phase-shift analysis coincide with each other.

3.3 Effect of ω − ρ meson coupling term in RMF model to parity-violating electron scattering

Lagrangian of RMF model:

$$
\begin{aligned}
\mathcal{L} \;=\; & \bar{\Psi}(i\gamma^{\mu}\partial\mu - M)\Psi && \mathcal{L}_N \\
& -\bar{\Psi}(g_{\sigma}\sigma + g_{\omega}\gamma^{\mu}\omega_{\mu} + \frac{g_{\rho}}{2}\gamma^{\mu}\boldsymbol{\tau}\cdot\vec{\boldsymbol{\rho}}_{\mu})\Psi && \mathcal{L}_{couple} \\
& -e\bar{\Psi}\gamma^{\mu}A_{\mu}\frac{e}{2}(1-\tau_3)\Psi - \frac{1}{4}F^{\mu\nu}F_{\mu\nu} && \mathcal{L}_{\gamma} \\
& +\frac{1}{2}\partial^{\mu}\sigma\partial_{\mu}\sigma - \frac{1}{2}m_{\sigma}^2\sigma^2 - \frac{\kappa}{3!}(g_{\sigma}\sigma)^3 - \frac{\lambda}{4}(g_{\sigma}\sigma)^4 && \mathcal{L}_{\sigma} \\
& -\frac{1}{4}\Omega^{\mu\nu}\Omega_{\mu\nu} + \frac{1}{2}m_{\omega}^2\omega^{\mu}\omega_{\mu} + \frac{\xi}{4!}(g_{\omega}^2\omega^{\mu}\omega_{\mu})^2 && \mathcal{L}_{\omega} \\
& -\frac{1}{4}\vec{R}^{\mu\nu}\cdot\vec{R}_{\mu\nu} + \frac{1}{2}m_{\rho}^2\vec{\rho}^{\mu}\cdot\vec{\rho}_{\mu} && \mathcal{L}_{\rho} \\
& +\Lambda_{\mathrm{v}}(g_{\rho}^2\vec{\rho}^{\mu}\vec{\rho}_{\mu})(g_{\omega}^2\omega^{\mu}\omega_{\mu}) && \mathcal{L}_{\omega\rho}
\end{aligned}
$$

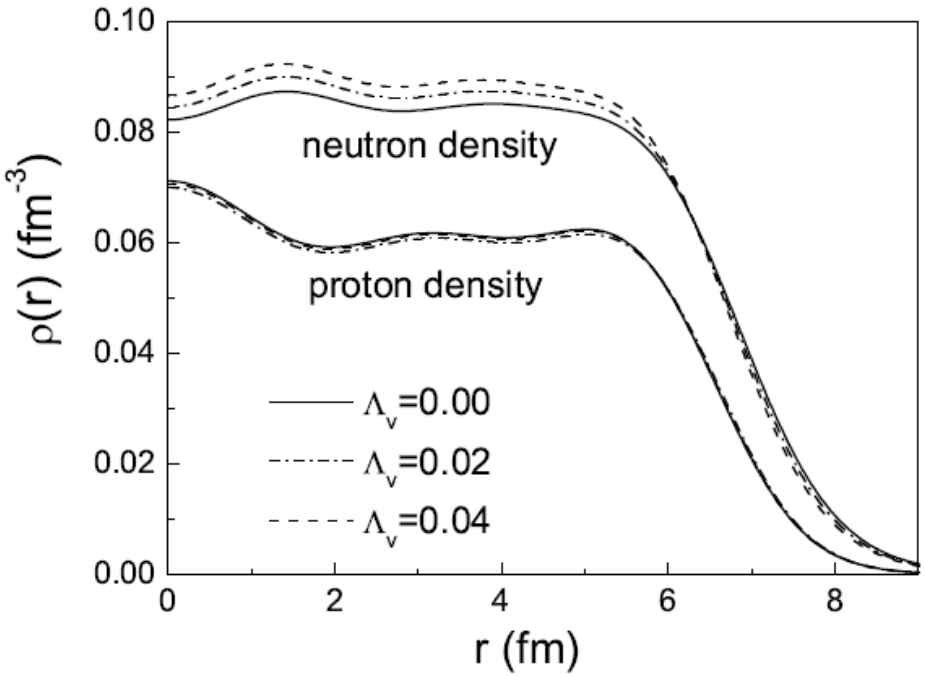

The proton and neutron densities of ^{208}Pb, which calculated from RMF model with different ω − ρ coupling term Λ_v.

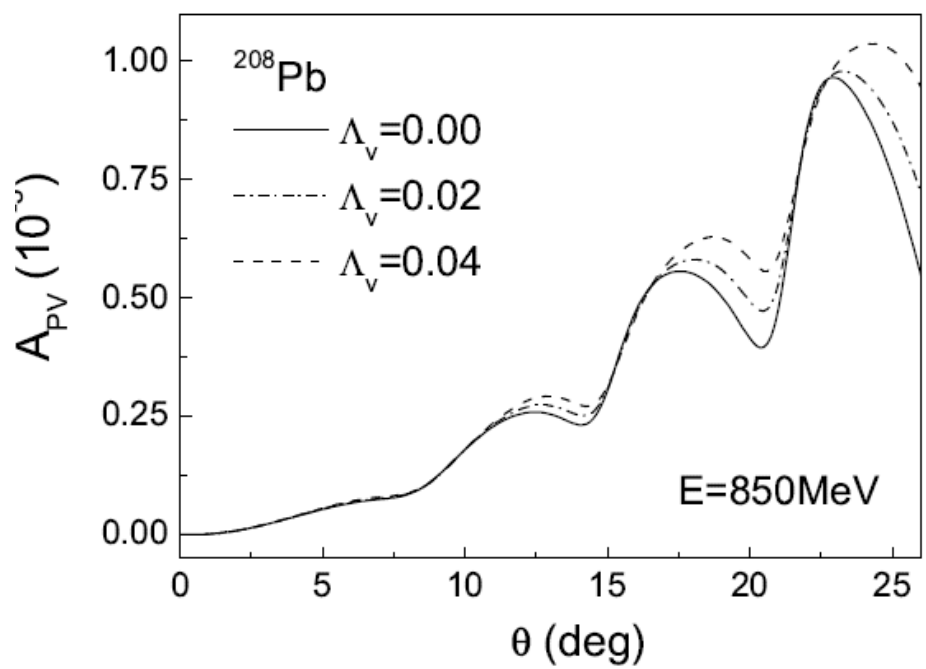

The Apv of ^{208}Pb for different ω − ρ coupling term Λ_v.

J. Liu and Z. Ren,
Phys. Rev. C **84**, 064305 (2011).

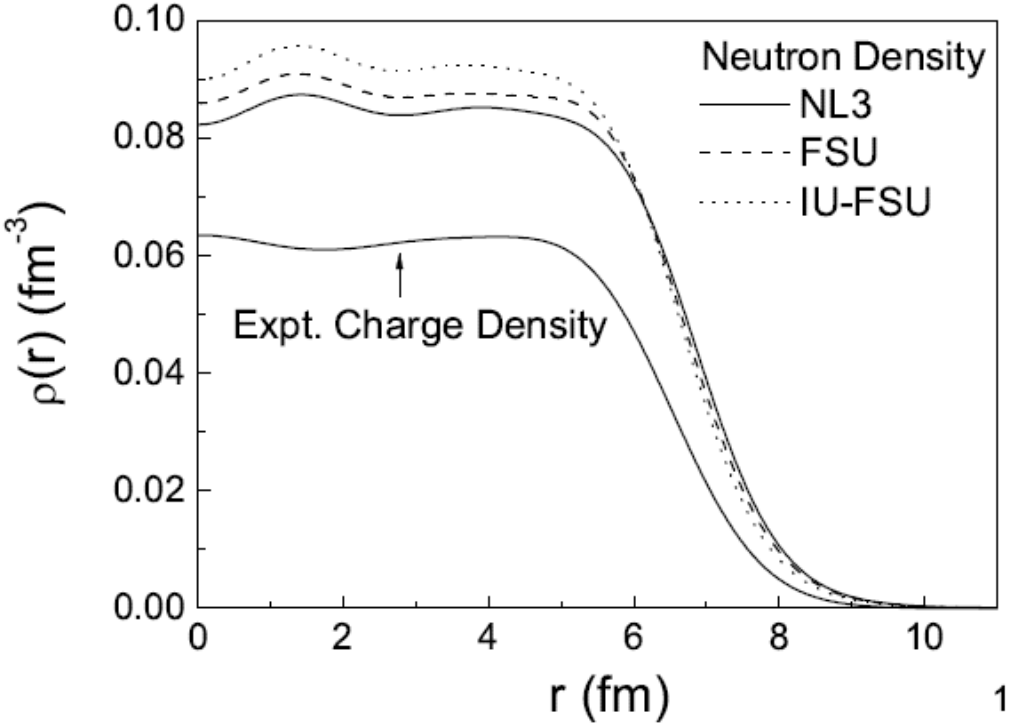

The neutron density distributions obtained from three different parameter sets.

J. Liu and Z. Ren,
Phys. Rev. C **84**, 064305 (2011).

Λv for different parameter sets

Model	Λ_v
NL3	0.00
FSUGold	0.030
IU-FSU	0.046

Apv of ^{208}Pb for different parameter set

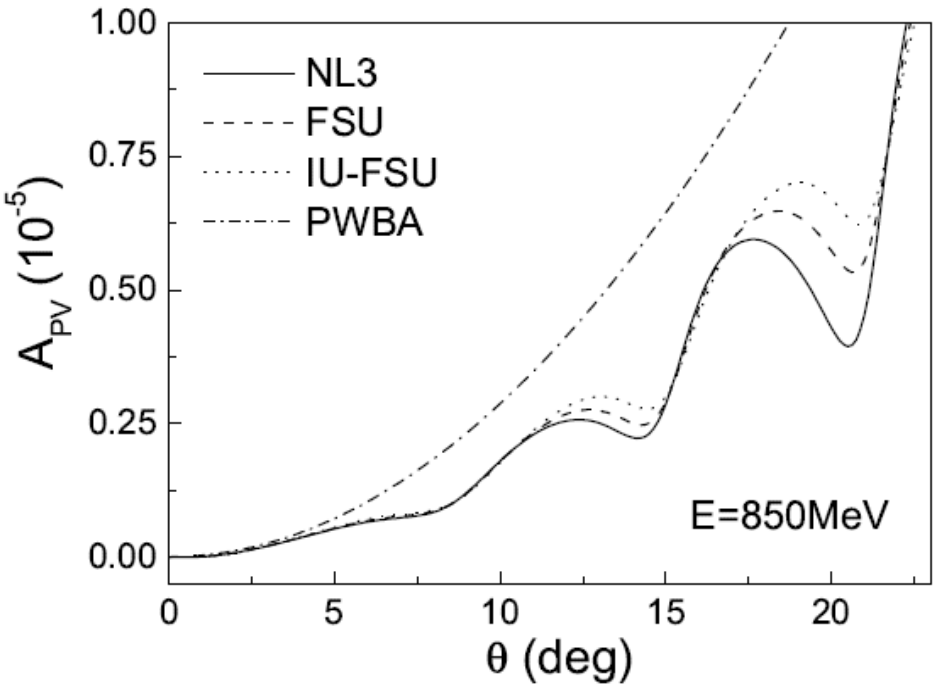

3.4 Statistical error of PVS measurement at different scattering angle

The assumption for extracting Rn:

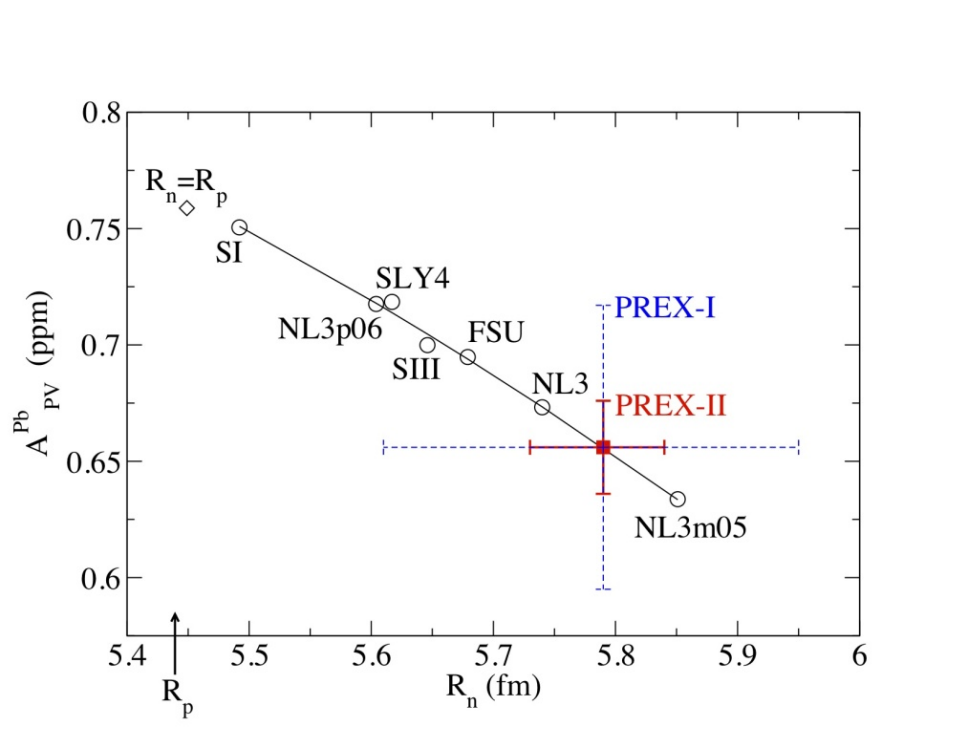

The relation between Apv and Rn

$$R_{np} = R_n - R_p = 0.33^{+0.16}_{-0.18} \text{ fm}$$

There are linear relation between Apv and Rn. Therefore, from one PVS measurement, the Rn can be extracted.

S. Abrahamyan et. al., *PRL* **108**, 112502 (2012)

Which scattering angle should be chosen?

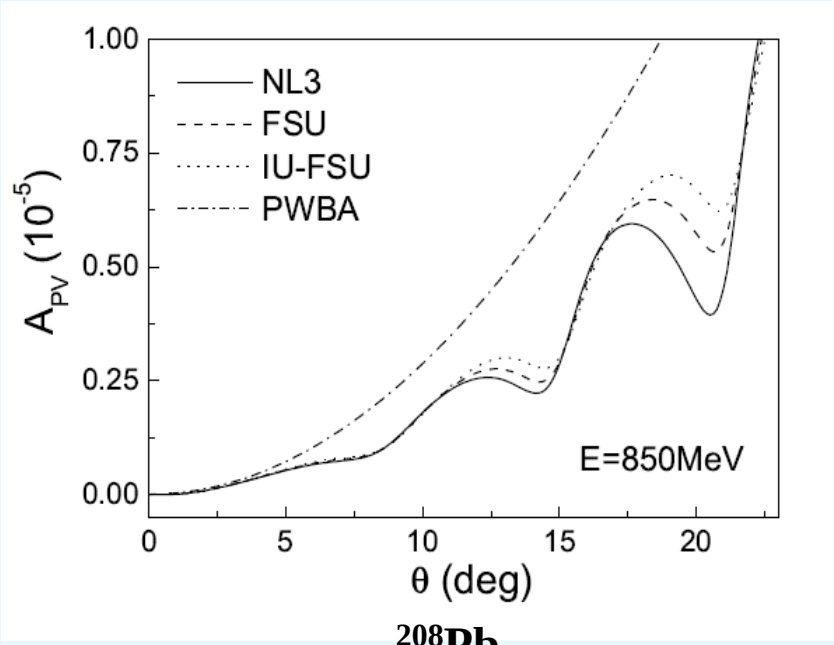

^{208}Pb

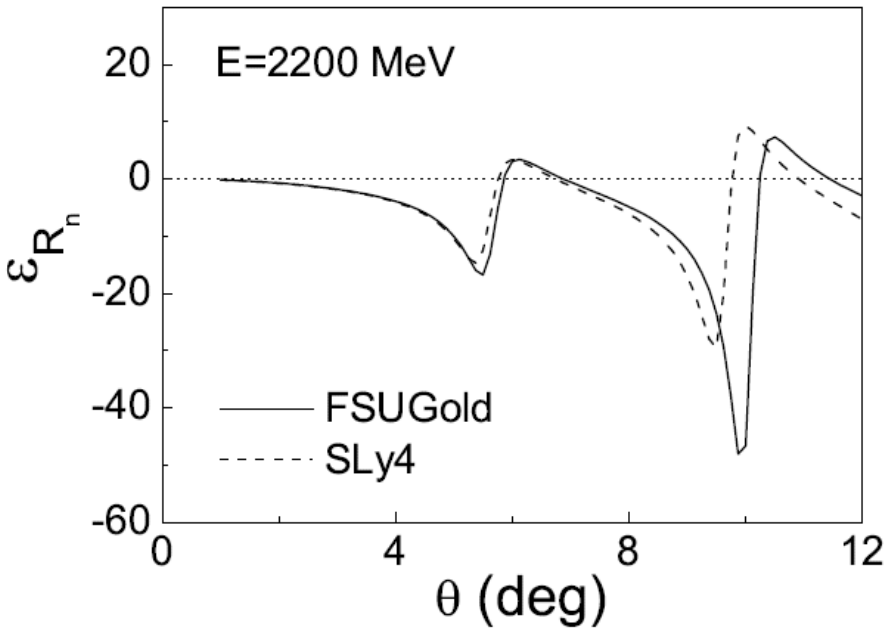

Sensitive of Apv to neutron radius Rn for ^{48}Ca

J. Liu and Z. Ren, *Nucl. Phys. A* **900**, 1 (2013).

The sensitivity of Apv to R_n :

$$\varepsilon_{R_n} = \frac{\mathrm{d}\ln A_{\mathrm{pv}}}{\mathrm{d}\ln R_n} = \frac{R_n}{A_{\mathrm{pv}}} \cdot \frac{\mathrm{d}A_{\mathrm{pv}}}{\mathrm{d}R_n}$$

The statistical error for measuring Rn:

$$\frac{\Delta R_n}{R_n} = \frac{1}{\sqrt{N_{\text{total}} A_{\text{pv}} P \varepsilon_{R_n}}}$$

$$N_{\text{total}} = I\, T \rho_{\text{tar}} \frac{d\sigma}{d\Omega} \xi\, \Delta\Omega\, N$$

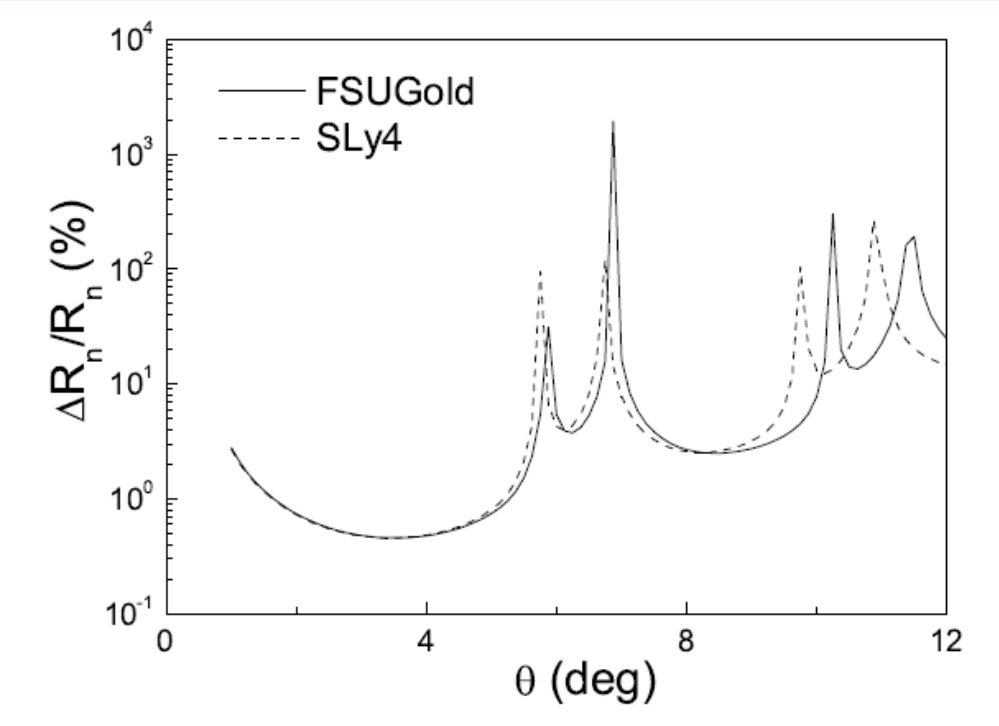

The statistical error of PVS for ^{48}Ca

Jefferson 实验室 PREx 以及 CREx 实验参数。

Parameters	I (μA)	E (GeV)	Angle	P	$\Delta\Omega$ (Sr)	N	ΔE (MeV)	t (cm)	ζ	A_{pv} (ppm)
PREx	100	1.05	5°	0.80	0.0037	2	4	0.05	0.34	0.6
CREx	100	2.20	4°	0.85	0.0016	2	4	1.00	0.34	2

3.5 Extracting the neutron density distributions by two PVS measurements

Density distribution in Droplet model:

$$\rho_i(r) = \frac{\rho_i^0}{1+\exp\left(\frac{r-C_i}{f_i t_i/4.4}\right)}, i = n, p$$

selecting condition: RMS radius, binding energy and δ_{np}.

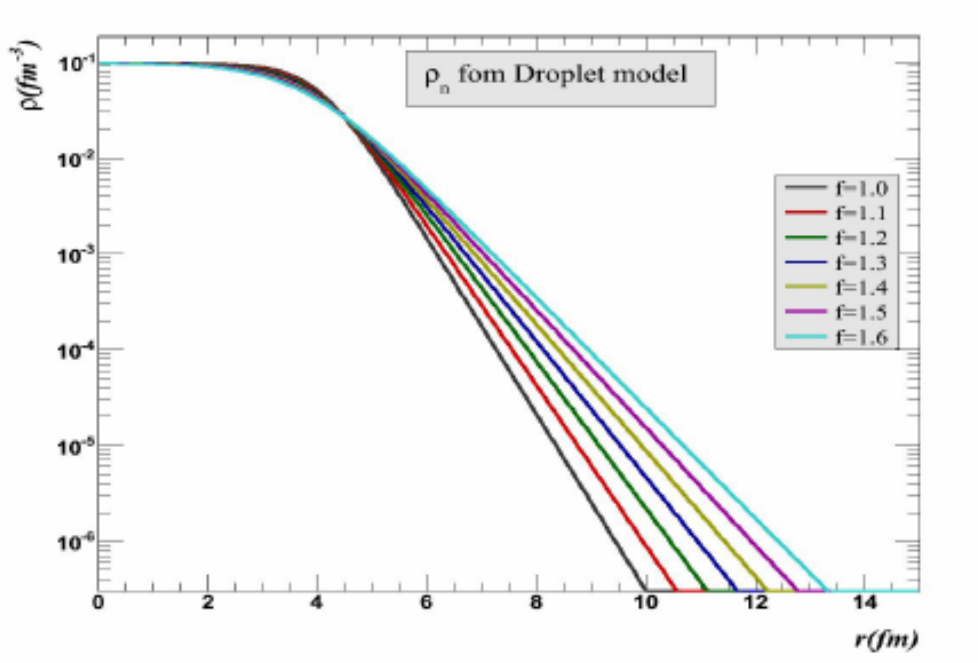

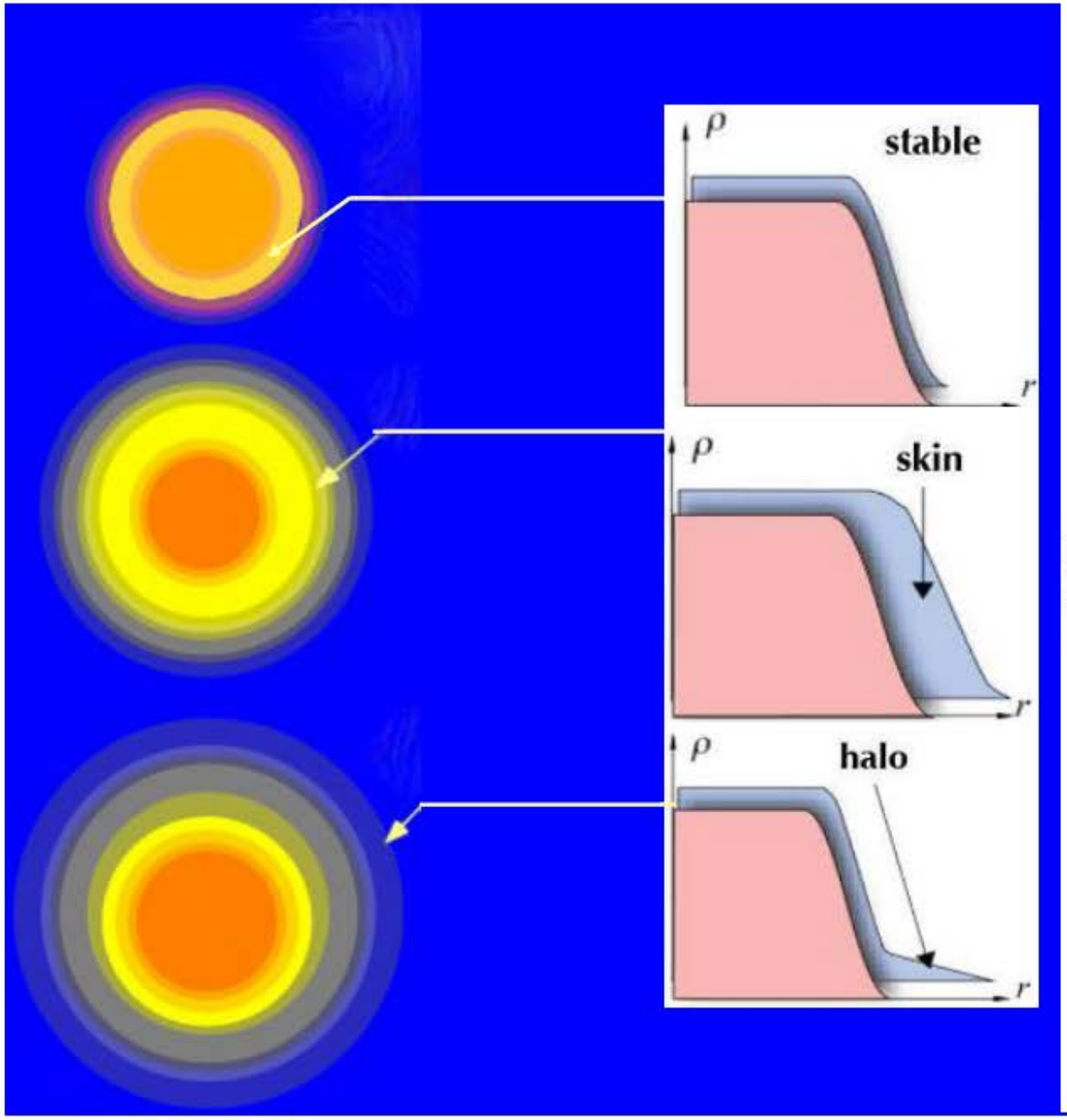
ρ
stable
r
ρ
skin
r
ρ
halo
r

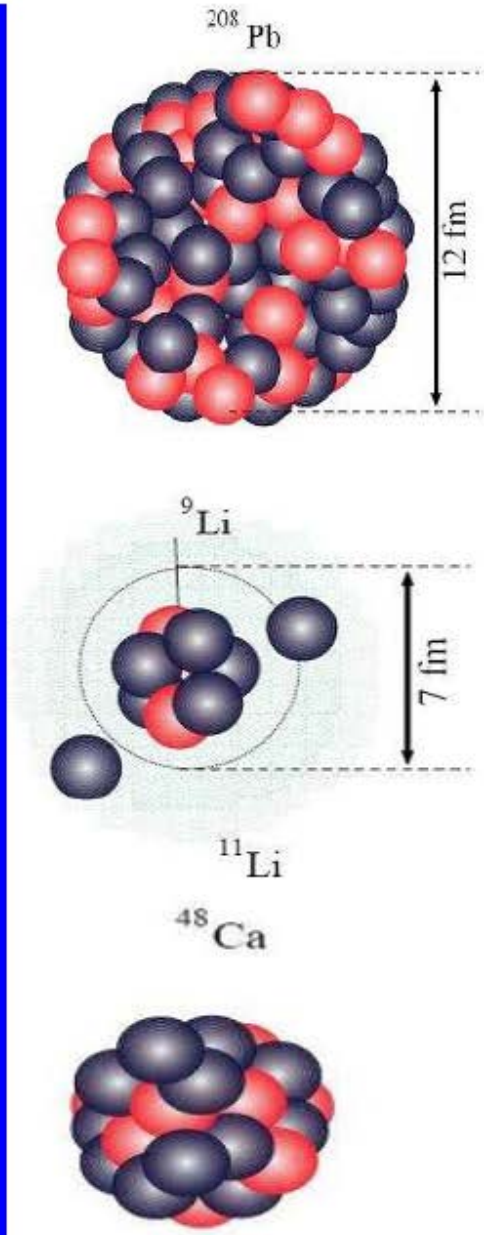
208 Pb
12 fm
9 Li
7 fm
11 Li
48 Ca

Supposing the neutron density distribution is the Helm model distribution,

$$\rho^H(r) = \int d\vec{r}' f_G(\vec{r} - \vec{r}')\rho_0 \Theta(R_0 - r)$$

where $f_G(r) = \left(2\pi\sigma^2\right)^{-3/2} e^{-r^2/2\sigma^2}$

$$A(r) = \frac{G_F}{2\sqrt{2}} \boxed{\rho_W(r)}$$

Weak charge density

The weak charge density can extracted by two PVS measurements:

Helm model has good analytical properties, whose form factors can be written as:

$$F^H(q) = \int e^{i\vec{q}\cdot\vec{r}} \rho^H(\vec{r}) d\vec{r} = \frac{3}{qR_0} j_1(qR_0)\, e^{-\sigma^2 q^2/2}$$

The analytic expression of radius of Helm model is:

$$\left\langle r^2 \right\rangle = \frac{3}{5}\left(R_0^2 + 5\sigma^2\right)$$

$$\left\langle r^4 \right\rangle = \frac{3}{7}\left(R_0^4 + 14R_0^2\sigma^2 + 35\sigma^4\right)$$

Statistical error for measuring σ_W

$$\frac{\Delta\sigma_W}{\sigma_W} = \frac{1}{\sqrt{N_{\text{total}} A_{\text{pv}} P \varepsilon_{\sigma_W}}} \qquad \varepsilon_{\sigma_W} = \frac{\mathrm{d}\ln A_{\text{pv}}}{\mathrm{d}\ln \sigma_W} = \frac{\sigma_W}{A_{\text{pv}}} \cdot \frac{\mathrm{d}A_{\text{pv}}}{\mathrm{d}\sigma_W}$$

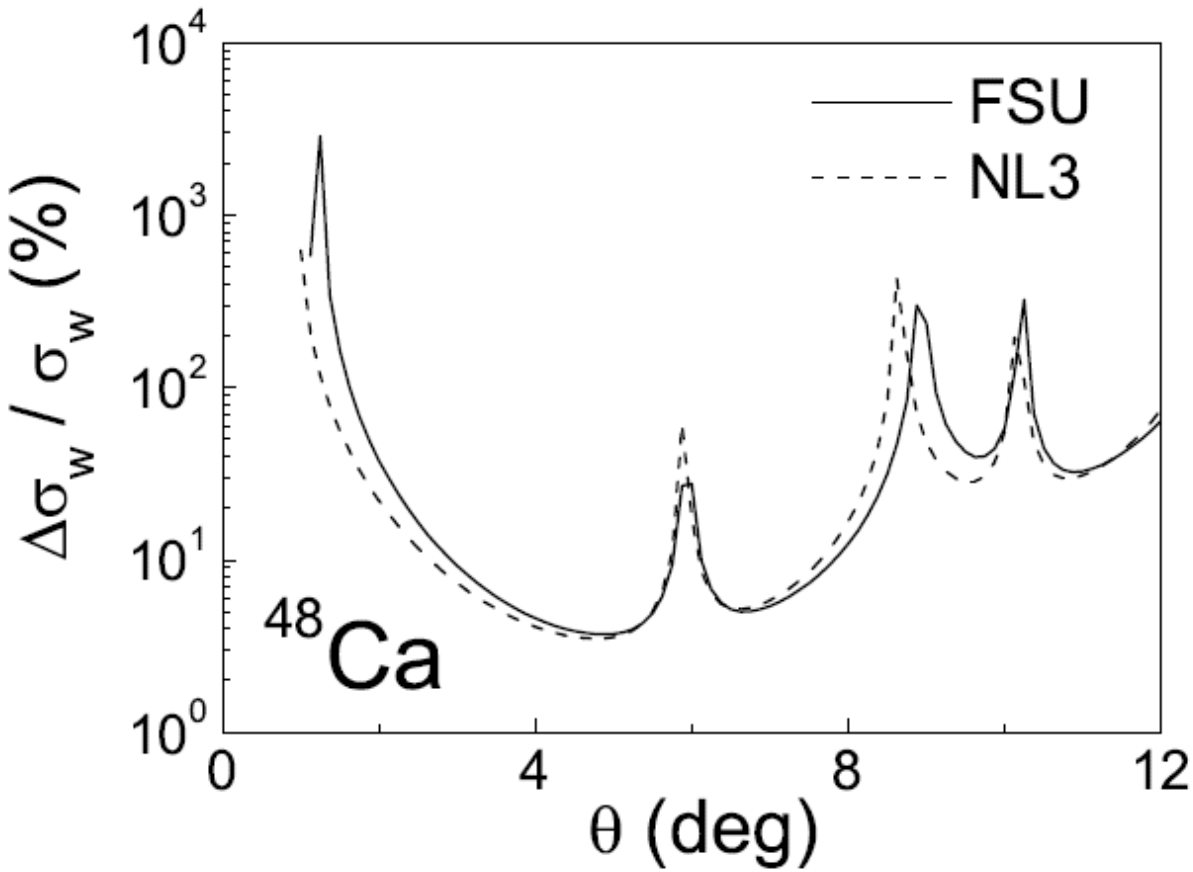

入射电子能量为2.2 GeV，实验时间为30 天。测量 ^{48}Ca 中子Helm 模型密度分布弥散系数σ_W 的误差。

J. Liu and Z. Ren, *Nucl. Phys. A* **900**, 1 (2013).

Under the PWBA method, we can obtain the relation between Apv and parameters of Helm model:

$$A_{PV} = \frac{G_F q^2}{4\pi\alpha\sqrt{2}} \frac{Q_{\mathrm{wk}} F_W(q)}{Z\, F_C(q)}$$
$$= k_0 + \alpha(R_{0\mathrm{W}} - R_{0\mathrm{C}}) + \beta(\sigma_W - \sigma_C)$$

$$k_0 = \frac{G_F q^2 Q_{\mathrm{wk}}}{4\pi\alpha\sqrt{2}Z} = 10.5\,\mathrm{ppm}$$

Then, take into account the Coulomb distortion corrections and calculate the Apv with the DWBA method again:

$$A_{\mathrm{pv}} = \frac{d\sigma_+ - d\sigma_-}{d\sigma_+ + d\sigma_-} = \frac{2\,\mathrm{Re}[M_\gamma^* M_Z]}{|M_\gamma|^2}$$

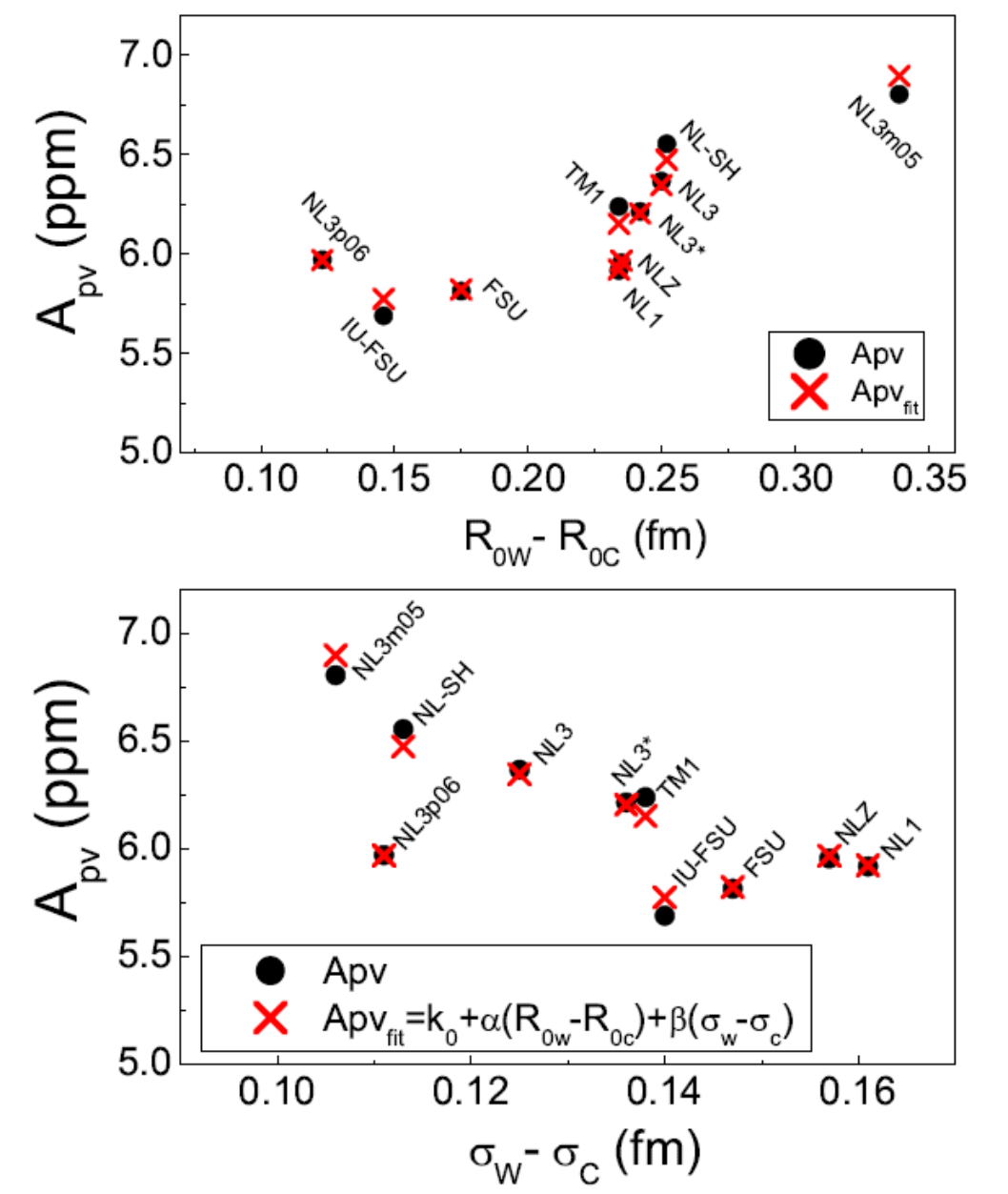

Apv of ^{48}Ca, calculated with the DWBA method

Fitting the theoretical results with:

$$A_{pv} = k_0 + \alpha(R_{0W} - R_{0C}) + \beta(\sigma_W - \sigma_C)$$

Though PWBA cannot give the accurate Apv, but it can give the relation between Apv and parameters of neutron distributions.

The results of DWBA also satisfy this relation.

J. Liu, Z. Ren, and C. Xu
Phys. Rev. C **88**, 054321 (2013).

Fitting the theoretical results from different parameter sets, we finally obtain:

$$A_{PV}(\text{ppm}) = 6.575 + 4.060(R_{0\text{W}} - R_{0\text{C}}) + 9.948(\sigma_W - \sigma_C)$$

(^{48}Ca, 6.5°)

Combining the weak skin thickness, the parameter of neutron density distribution can be extracted:

$$R_{\text{wskin}} = R_{\text{weak}} - R_{\text{ch}} = \sqrt{\frac{3}{5}\left(R_{0\text{W}}^2 + 5\sigma_{\text{W}}^2\right)} - R_{\text{ch}}$$

(^{48}Ca, 4°)

If the neutron density distribution is described by the two parameters distribution model, we can constrain the parameters by two PVS measurements at different angles.

J. Liu, Z. Ren, and C. Xu
Phys. Rev. C **88**, 054321 (2013).

Sec. IV Effect of nuclear deformation on electron scattering

The previous considered nuclei are the spherically symmetric. Most nuclei are found to be deformed in their ground states. The electric quadropole moments can be measured from experiments. Therefore we try to take into account the nuclear deformation during the studies of electron scattering.

The nuclear quadropole moment:

$$Q = \frac{1}{e}\int_V \rho_p(\mathbf{r})(3z^2 - r^2)d\tau$$

4.1 Deformed density distribution model

The spherical two-parameters Fermi (2pF) distribution:

$$\rho(r,\theta) = \rho_0 \left[1 + \exp\left(\frac{r-R}{a} \right) \right]^{-1}$$

Introducing the nuclear surface deformation, it can be rewritten as the deformed 2pF distribution:

$$\rho(r,\theta) = \rho_0 \left[1 + \exp\left(\frac{r-R(\theta,\varphi)}{a} \right) \right]^{-1}$$

$$R(\theta,\varphi) = R_0[1 + \beta_2 Y_{20}(\theta,\varphi) + \beta_4 Y_{40}(\theta,\varphi) + \cdots]$$

Multiply expanding the deformed 2pF model:

$$\rho(r,\theta) = \sum_L \rho^L(r) Y_{L0}(\theta)$$

$$= \rho^0(r) + \rho^2(r) Y_{20}(\theta) + \rho^4(r) Y_{40}(\theta) + \cdots$$

$\beta_l = 0$	$\beta_2 > 0$	$\beta_2 < 0$
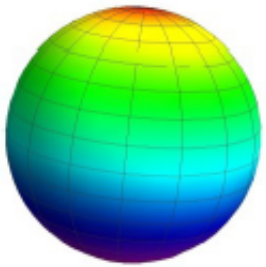	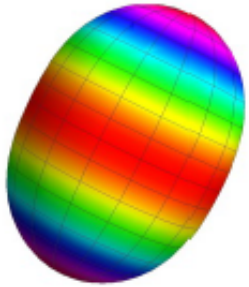	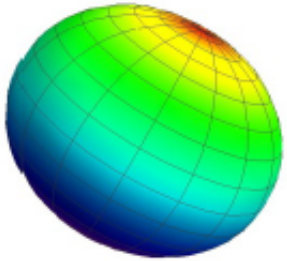
$\beta_3 \neq 0$	$\beta_4 \neq 0$	$\beta_2 >> 0$
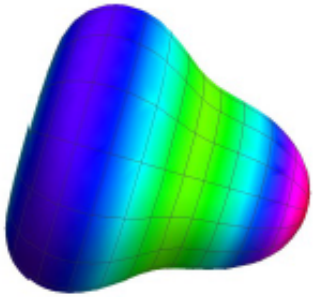	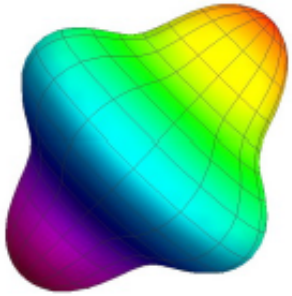	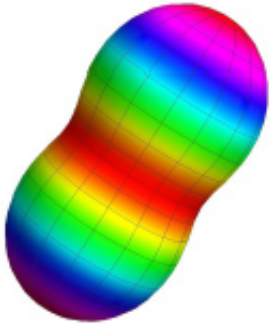

Nuclear surface shape for different L

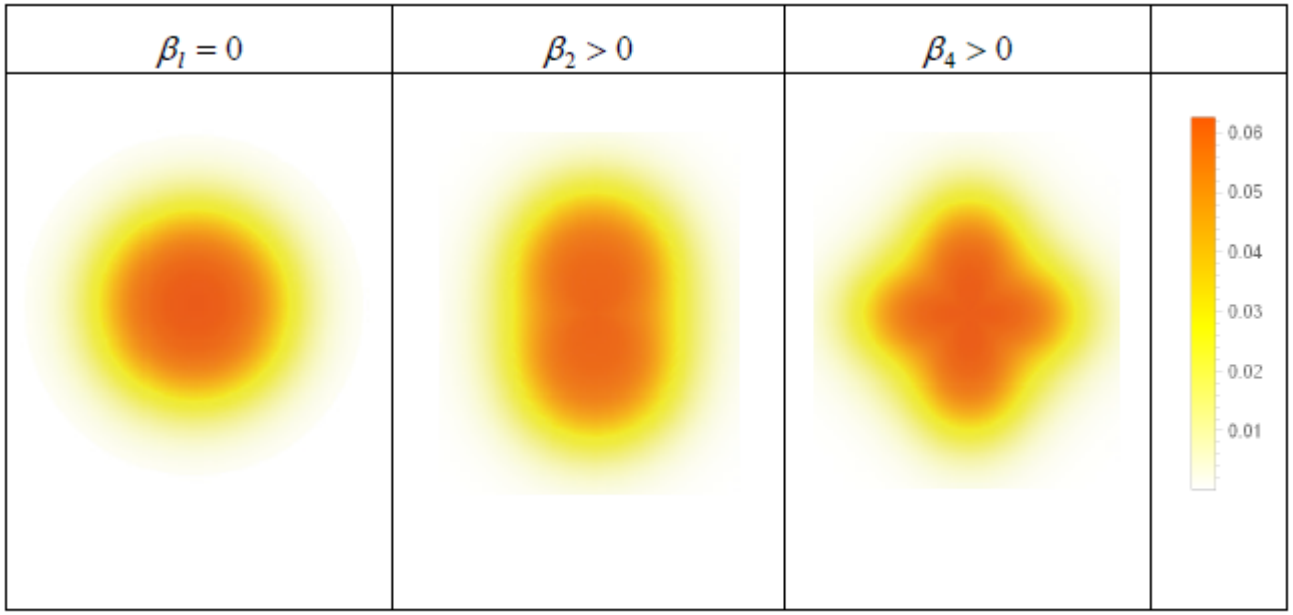

Nuclear proton density distribution for different L (Z=10)

The deformed nuclear density distribution can be written as the superposition of spherical part and deformed part:

$$\rho_p(\mathbf{r}) = \rho_p^0(r) + \rho_p^d(\mathbf{r})$$

Then we calculate the deformed nuclear density distribution from the RMF model.

In spherical RMF model:

$$\rho_p^0(r) = \sum_{i=1}^{A} (\frac{1}{2} - t_i)(|G_i(r)|^2 + |F_i(r)|^2)$$

The nuclear deformation is considered as the contributions of the proton hole in the outermost orbit.

$$\rho_p^d(\mathbf{r}) = \beta_d \frac{1}{r^2}(|G_j(r)|^2 + |F_j(r)|^2)(\frac{1}{4\pi} - |Y_{lm}(\theta,\varphi)|^2)$$

For example, there exists a proton hole in the $1p_{1/2}$ level for ^{14}N and in the $1d_{5/2}$ level for ^{27}Al.

$$|Y_{lm}(\theta,\varphi)|^2 = (-1)^m Y_{l,m} Y_{l,-m}$$

$$= (-1)^m \sum_L \left\{ \frac{(2l+1)^2}{4\pi(2L+1)} \right\}^{1/2} \langle lm, l-m | L0 \rangle \langle l0, l0 | L0 \rangle Y_{L0}$$

Deformed nuclear proton density distribution:

$$\rho_p(\mathbf{r}) = \rho_p^0(r) + \sum_{L=2}^{2l} \rho_p^L(r) Y_{L0}$$

$$\rho_p^0(r) = \sum_{i=1}^{A} (\frac{1}{2} - t_i)(|G_i(r)|^2 + |F_i(r)|^2)$$

$$\rho_p^L(r) = (-1)^m \beta_d \left\{ \frac{(2l+1)^2}{4\pi(2L+1)} \right\}^{1/2} \langle lm, l-m | L0 \rangle \langle l0, l0 | L0 \rangle \frac{1}{r^2} (|G_j(r)|^2 + |F_j(r)|^2)$$

4.2 Electron scattering off deformed nuclei

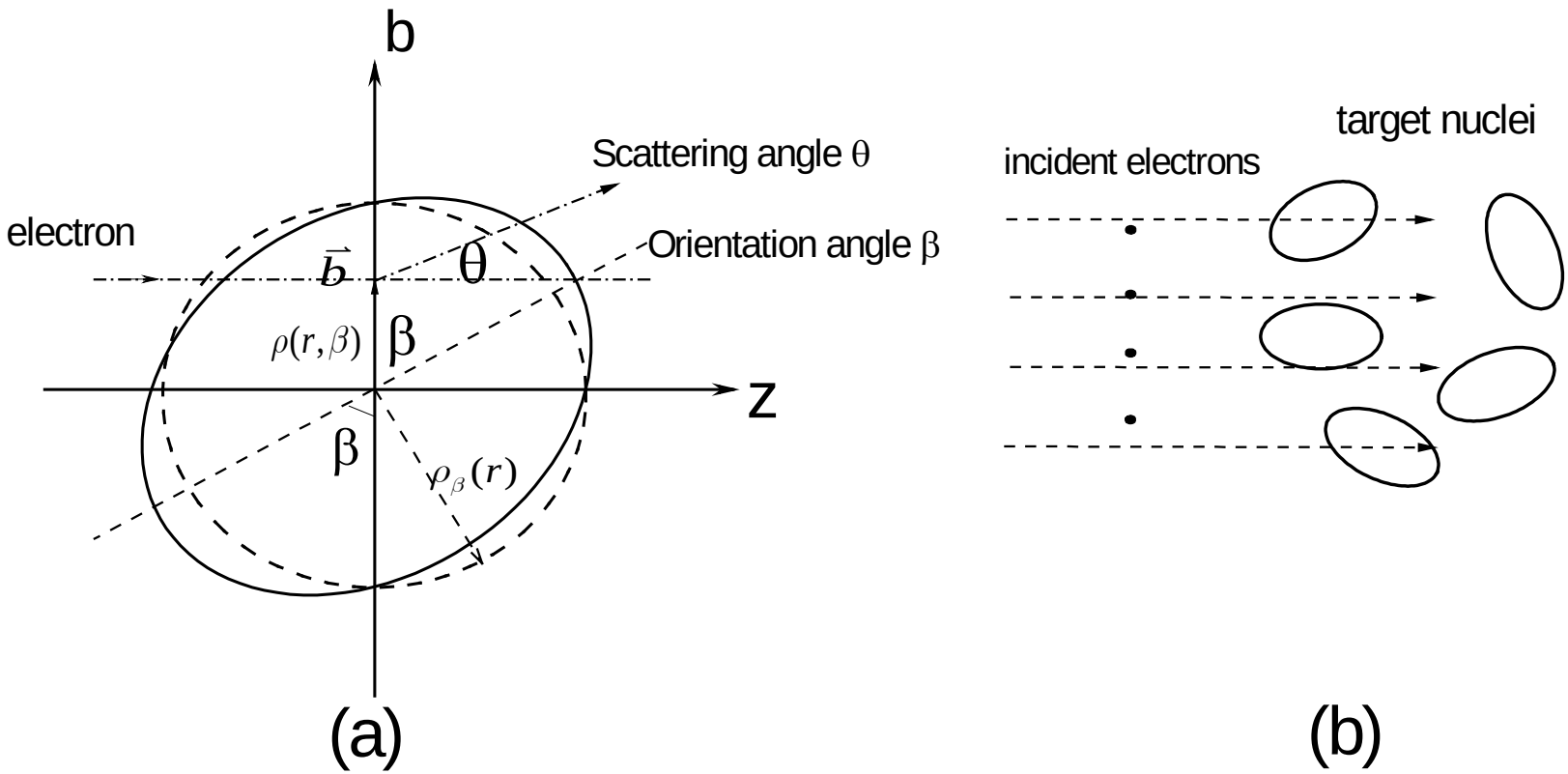

Sketch of electron scattering off deformed nuclei

The nuclear proton form factor under the PWBA:

$$F_p(q) = \frac{1}{Z}\int d^3 r \rho_p(\mathbf{r}) e^{i\mathbf{q}\cdot\mathbf{r}}$$

$$e^{i\mathbf{q}\cdot\mathbf{r}} = \sum_{L'} \sqrt{4\pi(2L'+1)} \cdot i^{L'} \cdot j_{L'}(qr) \cdot Y_{L'0}(\theta,\varphi)$$

$$\int_0^{2\pi} d\varphi \int_0^{\pi} d\theta \,\mathrm{Sin}\,\theta Y^*_{L'm'}(\theta,\varphi) Y_{Lm}(\theta,\varphi) = \delta_{L,L'}\delta_{m,m'}$$

$$|F(q)|^2 = F_{sphe.}(q)^2 + F_{defo.}(q)^2$$

$$= I_0(q)^2 + \frac{1}{2l+1}\sum_{m=-l}^{l}\left(\sum_{L=2}^{2l}(2l+1)\langle lm, l-m|L0\rangle\langle l0, l0|L0\rangle I_L(q)\right)^2$$

$$I_0(q) = \frac{1}{Z}\int d^3 r \rho_p^0(r) j_0(qr)$$

$$I_L(q) = \frac{1}{Z}\int dr j_L(r)(G_j^2 + F_j^2)$$

Taking into considerations of the Coulomb distortion effect:

$$|F_C(q)|^2 = F_{sphe.}^{DW}(q)^2 + \xi^2 F_{defo.}(q)^2$$

Finally, the scattering cross sections can be obtained:

$$\frac{d\sigma}{d\Omega} = \sigma_m \eta \frac{q_\mu^2}{q^2} F_C^2$$

the Mott cross section is $\sigma_m = \frac{Z^2\alpha^2 \cos^2\theta/2}{4E_i^2 \sin^4\theta/2}$

$$q_\mu^2 = q^2 - (E_i - E_f)^2$$

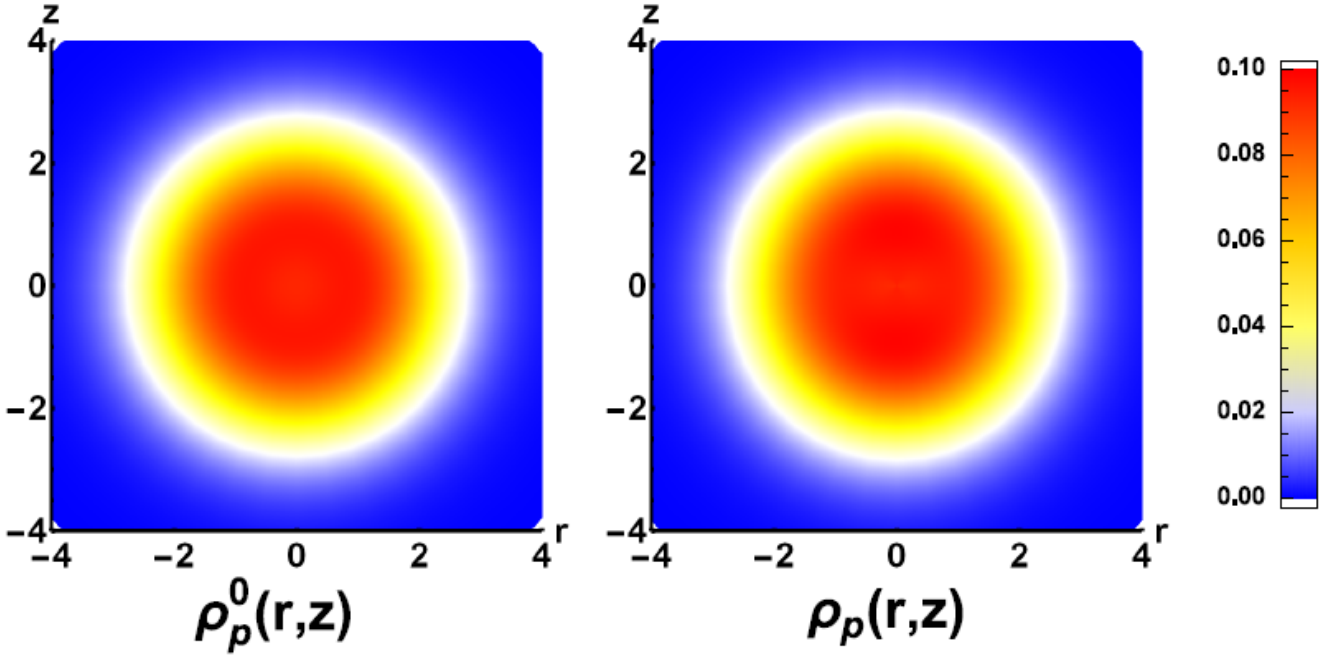

FIG. 1. Two-dimensional proton density distributions of ^{14}N in the $r-z$ plane of cylindrical coordinates, calculated with the FSU parameter set. $\rho_p(r,z)$ is the deformed proton density distribution calculated by the Eq. (8). $\rho_p^0(r,z)$ is the spherical part of the $\rho_p(r,z)$, which is calculated by the Eq. (4).

$$\rho_p(\mathbf{r}) = \rho_p^0(r) + \sum_{L=2}^{2l} \rho_p^L(r) Y_{L0}$$

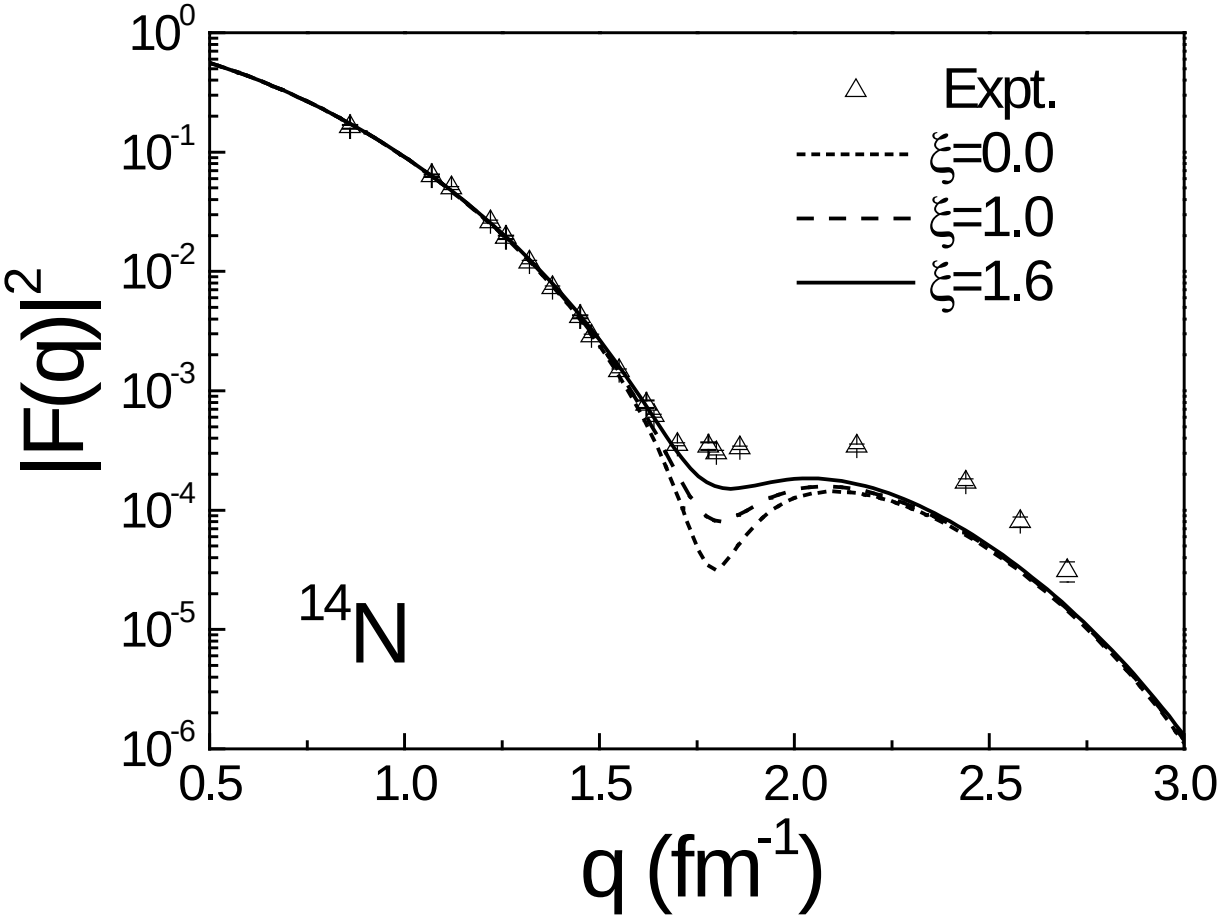

Nuclear charge form factors of ^{14}N

$$|F_C(q)|^2 = F_{sphe.}^{DW}(q)^2 + \xi^2 F_{defo.}(q)^2$$

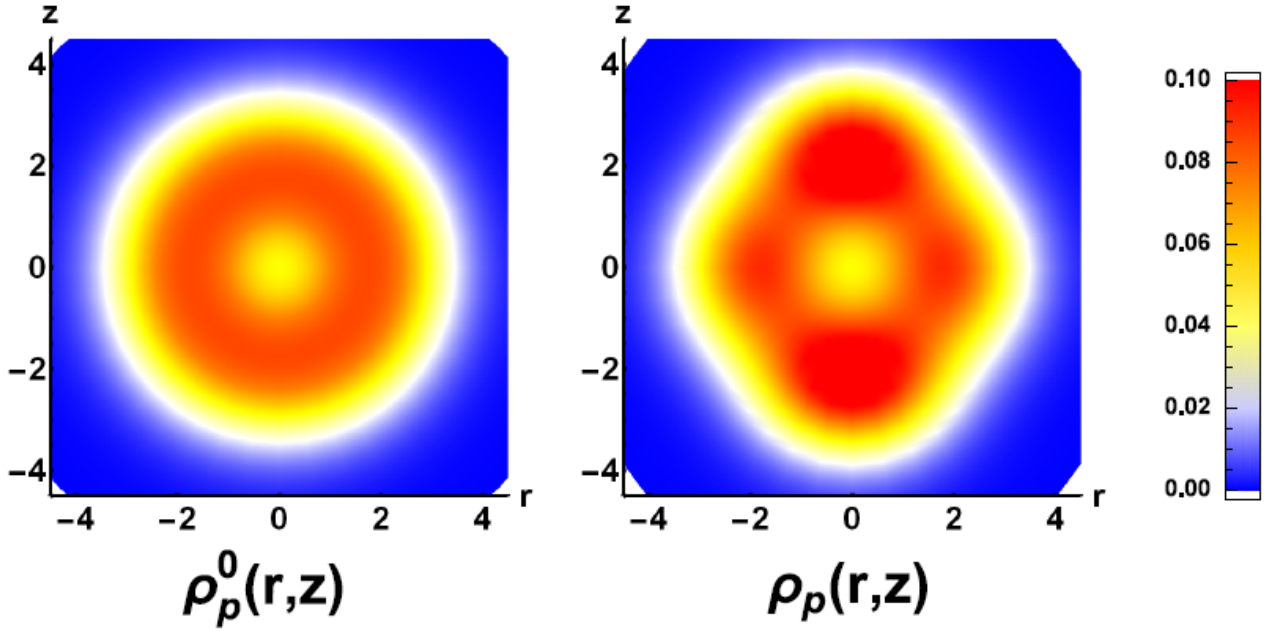

FIG. 4. Two-dimensional proton density distributions of ^{27}Al in the $r-z$ plane of cylindrical coordinates, calculated with the FSU parameter set. $\rho_p(r,z)$ is the deformed proton density distribution calculated by the Eq. (8). $\rho_p^0(r,z)$ is the spherical part of the $\rho_p(r,z)$, which is calculated by the Eq. (4).

$$\rho_p(\mathbf{r}) = \rho_p^0(r) + \sum_{L=2}^{2l} \rho_p^L(r) Y_{L0}$$

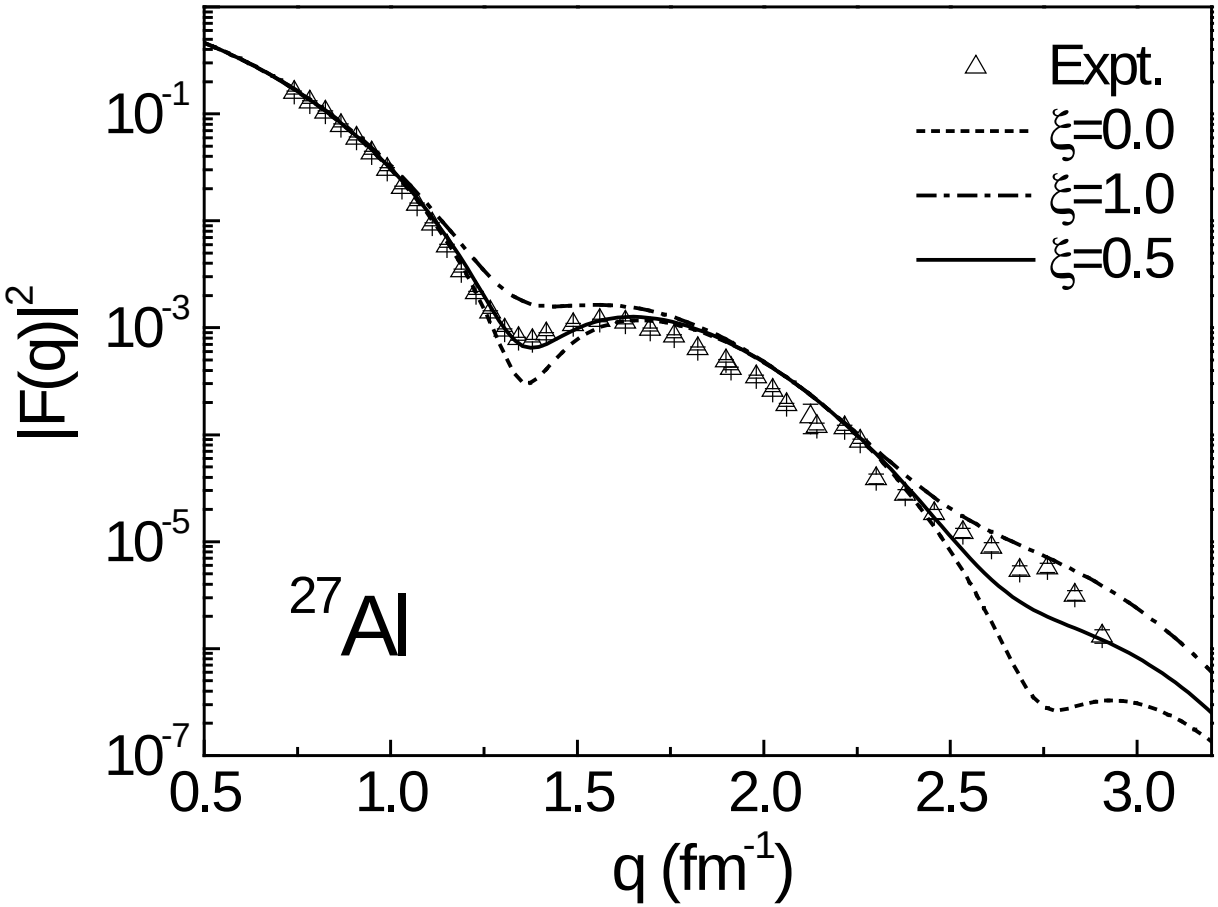

Nuclear charge form factor of ^{27}Al

$$|F_C(q)|^2 = F_{sphe.}^{DW}(q)^2 + \xi^2 F_{defo.}(q)^2$$

By including the nonspherical contribution in the scattering model, the theoretical results coincide with the experimental data much better. The introduction of the nonspheriacal contribution modifies the theoretical charge form factors at the positions of diffraction minima and high momentum transfers, but does not change the theoretical results at other positions.

This conclusion is obtained where the nuclear deformation is considered as the contribution of proton hole; however it is also applicable for other deformed nuclei. In the following work, we will further study electron scattering off deformed nuclei where the proton density distributions are obtained from the deformation-constrained mean-field calculations based on microscopic energy density functionals.

Summary

1. The parity-violating electron experiment is sensitive to the neutron density distribution. If the neutron density distribution is described by the two parameters distribution model, we can constrain the parameters by two PVS measurements at different angles.

2. The introduction of the nonspheriacal contribution modifies the theoretical charge form factors at the positions of diffraction minima and high momentum transfers, but does not change the theoretical results at other positions.


Thanks for your attention